NASA Earth Science Enterprise
Earth Science Applications Directorate
San Diego State University Affiliated Research Center

Interim Final Report:

The Utility of High Spatial Resolution Multispectral Imagery for Mapping and Monitoring Vernal Pool Habitat in Transitional Urban Environments

Project conducted by:
City of San Diego
202 C Street, M.S. 5a
San Diego, CA 92101

Report prepared by:
Keith Greer
City of San Diego, Planning Department

Lloyd Coulter and Allen Hope
San Diego State University, Department of Geography

Report prepared for:
Earth Science Applications Directorate
National Aeronautics and Space Administration
John C. Stennis Space Center, Mississippi 39529

9/27/02

Table of Contents

Tables

Figures

Executive Summary

Vernal pools are seasonal, depression-type wetlands which function as micro-habitats that support multiple rare, threatened and endangered species. Vernal pools largely occur on tops of mesas within the western half of San Diego County. Due to decades of expansive urban development, only 5% of the original vernal pool population exists today and many of the remaining pools are severely degraded and are at risk of being destroyed. Vernal pools are now considered sufficiently critical that local, state and federal laws require the protection of vernal pools even when they occur on private property. Successful stewardship of vernal pools is dependent on the ability to locate and monitor the status of the pools and the species that occur within them. Currently, the management and monitoring of vernal pools is performed through field surveys which is time consuming, costly, and limited in spatial coverage. Remote sensing offers the opportunity to derive valuable habitat information at spatial and temporal scales that are not possible with ground sampling.

The utility of high spatial resolution, multispectral imagery was evaluated for multiple tasks associated with vernal pool mapping and characterization, including: locating unknown pools and delineating pool basin extents, mapping vernal pool plants, estimating pool depth, and characterizing land use and land cover adjacent to sensitive vernal pool habitats. ADAR 5500 multispectral imagery was acquired at multiple resolutions within two San Diego County study sites during February and May of 2001. The first site at Otay Mesa was reconstructed in 1998 as part of a land mitigation project and contains over 300 vernal pools within a small geographic area. Naturally occurring pools in this area were scraped and destroyed in the 1970s. The second site at Marron Valley contains a small number of naturally occurring vernal pools. This site is the subject of biological monitoring, as recent fires and many years of cattle grazing have degraded the habitat surrounding the vernal pools.

An experiment was performed with multiple resolutions of imagery at both study sites to determine to optimum spatial resolution for identifying and delineating vernal pools. One foot resolution image mosaics at each site were aggregated to simulate 2 ft, 4 ft, 8 ft, and 16 ft spatial resolutions. Nine interpreters visually identified apparent vernal pools beginning with the lowest resolution imagery and then with progressively higher spatial resolution imagery. The number of pools correctly identified and the number of pools falsely identified were tallied up and analyzed. Results from the analysis suggest that 2 ft resolution imagery is optimum detecting pools. It is estimated that water filled pools can be delineated with 2 ft to 4 ft precision, using 2 ft resolution multispectral imagery. Delineation of dry pool basins is expected to have lower precision. In all cases, pool identification and delineation is influenced by pool size, color, contrast to background, and vegetation within and surrounding the pools.

The utility of high spatial resolution, multispectral imagery for mapping vernal pool plants was assessed. Vernal pool plants were classified through unsupervised and supervised image classification using 2 inch resolution ADAR 5500 imagery acquired in May of 2001. A reference map derived through field-based delineation of vernal pool plants onto hardcopy image plots in June and August of 2001 was utilized to validate the image classification products. *Eryngium*

aristulatum and *Eliocharis macrostachya* classified with 60% to 75% accuracy. Classification accuracy was lower for other plants included in the analysis. In conjunction with the image classification analysis, spectral characteristics of vernal pool plants were summarized.

The depth of water within vernal pool basins significantly affects the abundance and diversity of plants and invertebrates that pools may support in a given season. To determine if high spatial resolution multispectral imagery could be utilized to estimate pool depth, three indices were generated from the February imagery and compared to field collected depth measurements at the Otay Mesa site. Relationships between water depth and the spectral index products evaluated were found to be weak or non-existent.

The greatest utility of remote sensing for vernal pool management is likely to be in locating and mapping vernal pools and in documenting and characterizing land cover conditions within and adjacent to the pools. However, the utility of remote sensing for deriving relevant information is also a function of cost associated with mapping through remote sensing. If the remote sensing approach is to be implemented, it must be cost-effective relative to alternative methods of locating and delineating unknown vernal pools, such as field-based mapping. A comparative analysis of image-based and field-based mapping was performed to assess the relative cost-effectiveness of the two approaches. Results from the analysis indicate that mapping vernal pools over extents of several kilometers is likely to be most cost-effective through remote sensing.

1.0 Introduction

Vernal pools are seasonal, depression-type wetlands which function as micro-habitats that support multiple rare, threatened and endangered species. Vernal pools have been recognized explicitly as an important habitat resource since 1979 when the first resource inventory was completed for the State of California (Beauchamp, 1979). Vernal pools largely occur on tops of mesas within the western half of San Diego County. These mesas are considered prime urban development sites due to the ease of construction. After decades of expansive urban development, only 5% of the original vernal pool population exists today (Bauder 1986; Bauder 1987; and Bauder and McMillan 1998). Many of the remaining pools are severely degraded and are at risk of being destroyed (Bauder 1986; Bauder 1987; and Bauder and McMillan 1998). Vernal pools are now considered sufficiently critical that local, state and federal laws require the City of San Diego (City) to protect vernal pools within their jurisdiction, even when they occur on private property. Consequently, vernal pool environments are now the subject of intense mitigation, preservation, and restoration. Recent protection and management programs include the San Diego National Wildlife Refuge Vernal Pool Stewardship Project (U. S. Fish and Wildlife Service, 1997) and the Multiple Species Conservation Program (MSCP) (City of San Diego et al., 1997).

The MSCP is a multi-agency program designed to build and manage a county-wide habitat preserve, within the jurisdiction of the City of San Diego. Within the City of San Diego Planning Department, the staff of the MSCP are tasked with implementing a regional conservation plan designed to preserve the City's habitat and open space, protect its bio-diversity and enhance the quality of the City's environmental resources. The City has completed planning efforts to identify core biological resource areas targeted for conservation and has entered into an agreement with the federal and state wildlife agencies to ensure implementation of the resource conservation plan and habitat preserve. Current efforts of the City MSCP staff largely focus on preserve assembly, management and monitoring. Critical among the environmental resources under the protection of the City are vernal pools. The City MSCP staff is actively seeking improved methods for mapping and monitoring vernal pools and has asked the San Diego State University (SDSU) Affiliated Research Center (ARC) program for assistance.

Successful stewardship of vernal pools is dependent on the ability to locate and monitor the status of the pools and the species they support. Remnants of the vernal pool population are known to exist on both public and private lands, but are not well mapped or characterized. Therefore, they are subject to indirect harm by off-road vehicles and benign neglect. Mapping and monitoring these pools is essential to establishing a baseline for monitoring future changes that may impact these valuable resources.

Currently, the management and monitoring of vernal pools is performed through field surveys which is both time consuming and costly. Field surveys are also limited in that they only allow sampling of variables such as pool size, water depth and duration, plant species diversity and cover density, surrounding land use, and general hydrologic flow patterns at infrequent time intervals. Such sampling is often spatially and temporally limited and does not provide a synoptic coverage of the condition of entire complexes occurring at multiple locations within the City. Remote sensing offers the opportunity to derive valuable habitat information at spatial and temporal scales that are not practical through ground surveys. In addition, remote sensing can provide the ability to comprehensively quantify resources and develop a library of historic imagery for change detection efforts.

2.0 Project Objectives

Locating and mapping all vernal pools within the City of San Diego is an important first step in protecting these pools and advocating stewardship of those located on private lands. At present, the City estimates that only 80% of the vernal pools within the city are known to exist. In addition to locating the vernal pools, it is necessary to characterize the condition of these pools by quantifying such things as plant diversity, plant abundance, pool area and depth, and condition of surrounding landscape. Further, it is critical to the success of any remote monitoring program to be cost effective.

The overall goal of this project was to assess the utility of high spatial resolution, multispectral imagery for mapping and monitoring vernal pool locations, extents, plant diversity and density, and surrounding land cover variables that are central to characterizing the condition of the pools and the species that they support. The primary objectives were to: 1) determine the optimum spatial resolution at which multispectral imagery should be acquired to enable accurate identification and delineation of unknown vernal pools in the most cost effective manner; and 2) indicate the spectral separability of vernal pool plant species and the potential accuracy with which they may be mapped using broadband, multispectral imagery acquired with high spatial resolution.

Secondary objectives were to: 1) assess any correlation between spectrally derived products and measures of water depth; and 2) indicate the utility of multispectral imagery for mapping land covers and land uses within the landscape surrounding vernal pools which relate to pool health. These include variables such as vegetation community type, local disturbance, urban land use, mima mounds, and watershed boundaries.

3.0 Study Area and Data

3.1 Study Area

Two areas containing assemblages (i.e., complexes) of vernal pools were selected as study sites for this project (Figure 1). The first site at Otay Mesa contains vernal pools reconstructed in 1998 as part of a habitat mitigation. Naturally occurring pools in this area were scraped and destroyed in the 1970s. This site was selected because it contains over 300 pools densely located within a small geographic area and because monitoring of the health and successful development of these pools is an ongoing requirement of the mitigation.

The second site located within Marron Valley contains a small number of naturally occurring vernal pools. This site is also the subject of biological monitoring, as recent fires and many years of cattle grazing have degraded the habitat surrounding the vernal pools. The cattle were permanently removed in March of 2002, and the City of San Diego will begin to monitor the recover of this landscape. The Marron Valley site was specifically chosen for this project in order to evaluate the utility of high resolution, multispectral imagery for detecting naturally occurring vernal pools.

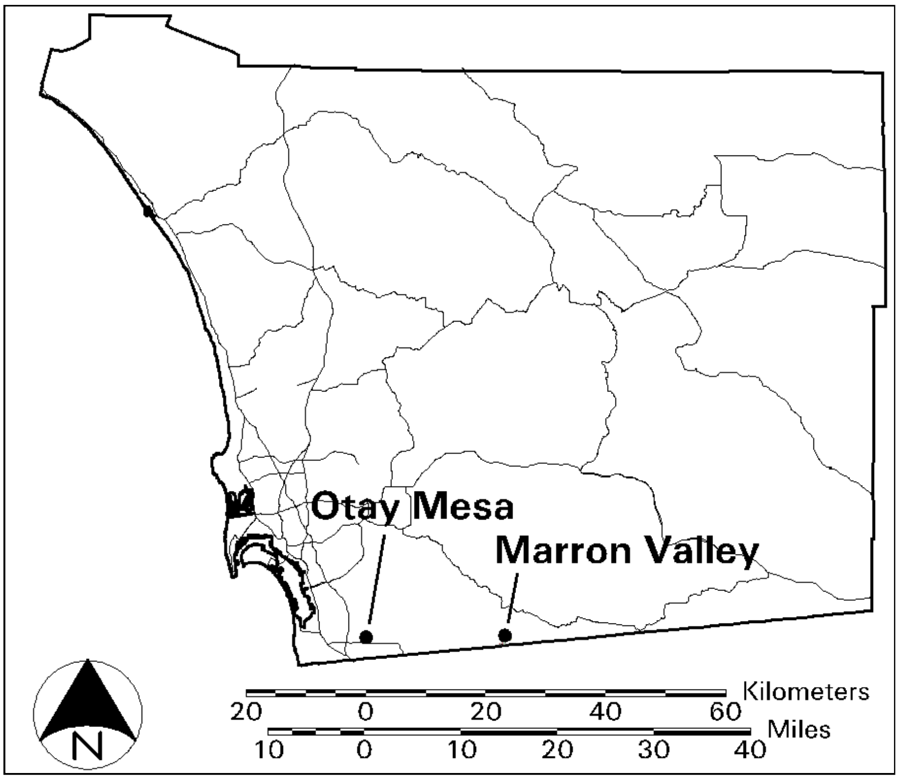

Figure 1. Otay Mesa and Marron Valley study sites within San Diego County.

3.2 Data

ADAR 5500 imagery acquired from a helicopter platform in February and May of 2001 at the Otay Mesa and Marron Valley sites were the primary data sets analyzed during this project. The ADAR 5500 is a four digital camera multispectral imagery system which acquires imagery in the blue (450-540 nm), green (520-600 nm), red (610-690 nm), and near-infrared (NIR) (780-1000 nm) wavebands. Imagery at Otay Mesa was acquired at 1 foot spatial resolution on February 2nd, 2001 and at 1 foot and 2 inch resolution on May 23rd. Imagery at Marron Valley was acquired at 1 foot resolution on February 2, 2001. The February 2nd imagery was captured five days after the second of two major rain events within a two week period. The timing of the acquisition was near optimal for capturing vernal pool basins filled with water. At this time, the pool basins had little or no plants established within them. The May 23rd acquisition was near the peak of the growing season of vernal pool plants. At this time, most pools were not ponding water and the pools contained the greatest plant diversity and abundance of the season. Selected frames from each site were georeferenced using a 2000 color-infrared digital orthophotographic mosaic as a registration base. Image mosaics were then created for each image set at the Otay Mesa and Marron Valley sites. In addition to the ADAR 5500 airborne imagery, IKONOS panchromatic satellite imagery at 1 m spatial resolution was extracted from the SDSU archive and reviewed. The IKONOS imagery covered Del Mar Mesa, an area outside the primary study sites of this project.

Field reconnaissance was performed following the flights to document scene conditions and to generate reference data for validation of image-derived products. Following the February 2nd acquisition, representatives from the Department of Geography at SDSU and the City of San Diego visited the Otay Mesa site on February 5th and recorded pool depths and general pool turbidity, and captured photographs to document pool conditions. Following the May 23rd flight, representatives from the City and SDSU visited the Otay Mesa site on June 7th and delineated polygons of homogenous vegetation onto large-scale, hard copy plots of 2 inch resolution ADAR 5500 images acquired on May 23rd and captured photographs documenting pool and vegetation cover conditions. Hard copy plots were also taken into the field on August 17, 2001 in an attempt to examine correlation between particular spectral properties and individual vernal pool plant species. The plants were senesced at the time, but patterns of spectral characteristics were still able to be linked to individual plant species in many instances. Field reconnaissance was also performed at Marron Valley to provide reference information on the locations of vernal pools at that site.

A reference vegetation map was generated from the vegetation polygons and individual plants delineated on hardcopy image plots during the June and August field work campaigns at Otay Mesa. This map was created by heads-up digitizing the vegetation polygons onto a raster image backdrop and then coding the vegetation classes into a new thematic raster image. The resulting thematic raster image precisely matched the 2 inch resolution ADAR 5500 image mosaic both in terms of cell size and spatial position.

Plants mapped during the June and August field campaigns are summarized in Table 1. The total area of each reference class used to validate image classifications and its relative proportion of the total area mapped are also provided in Table 1. It is clear that many vegetation types represented a small proportion of the total area of vegetation mapped in the field. Some polygons delineated in the field were mapped as mixtures of two or more vegetation types. These polygons could not be utilized to validate image classifications of vegetation type and are not included below as a percentage of the total mapped area. *Juncus bufonius* (Jubu) was noted as being present in some of the polygons mapped in the field as mixed, but was not mapped as a homogenous polygon. Therefore, the Jubu class was not included in the reference vegetation map. The name aster is used to describe an unidentified sunflower within the Otay Mesa vernal pool site. The few occurrences of *Viguiera lacinata* (Vila), aster, and *Hemizonia fasciculata* (Hefa) were outside the vernal pools and were not considered during the image classifications. However, spectral signatures were evaluated for these plant types.

Table 1. Plants mapped at the Otay Mesa vernal pool site.

Code	Scientific Name	Common Name	Area (square meters)	Percent of Mapped Area
Erar	Eryngium aristulatum	button celery	549	71.32%
Ponu	Pogonyne nudiuscula	Otay Mesa mint	11	1.46%
Elma	Eliocharis macrostachya	spike-sedge	145	18.81%
Jubu	Juncus bufonius	toad rush	0	0.00%
Psbr	Psilocarphus brevissimus	wooley marbles	54	7.04%
Lisc	Lilaea scilloides	flowering quillwort	5	0.70%
Plac	Plagiobothrys acanthocarpus	adobe popcornflower	5	0.66%
Vila	Viguiera lacinata	San Diego sunflower	6	---------
Aster	Aster		1	---------
Hefa	Hemizonia fasciculata	tarplant, tarweed	24	---------
Mixed			277	---------

A range of vernal pool plant species were field mapped and included in the reference layer. *Eryngium aristulatum* (Erar) and *Pogonyne nudiuscula* (Ponu) are listed as endangered species. The presence of Erar plants indicates that a pool has had a short duration of inundation. In addition, Erar plants indicate that other endangered plants are likely to be present in the pool, as approximately 25% of pools with Erar also support other endangered species. The presence of *Eliocharis macrostachya* (Elma) indicates that a pool has been ponding water for a relatively long duration and will support flora with similar inundation duration requirements. *Psilocarphus brevissimus* (Psbr) plants are particularly useful as an indicator that a vernal pool is actually present.

In addition to the field reference data collected by the City and SDSU, pool boundary and contour maps provided by the City were available to assess pool extent and micro-topography characteristics such as mima mound locations and drainage patterns. Mima mounds are characteristic mound features found within vernal pool environments. The contour data were reviewed in conjunction with the imagery to identify any correspondence between micro-topography in and around the vernal pools and features apparent in the imagery.

4.0 Methods

4.1 Optimum Spatial Resolution for Pool Detection and delineation

Imagery acquired with 1 ft spatial resolution at Otay Mesa and Marron Valley during February was exploited to determine the optimum spatial resolution at which broadband multispectral imagery should be acquired in order to first detect and second delineate vernal pools imaged during wet season. Multiple images with decreasing spatial resolution were generated from the

1 ft resolution Otay Mesa and Marron Valley mosaics. Simulated spatial resolutions were 2 ft, 4 ft, 8 ft, and 16 ft. The geographic extent of the Otay Mesa and Marron Valley test sites are 7 and 75 hectares, respectively. The Otay Mesa test site contains 125 pools densely located within a relatively small area, while the Marron Valley test site contains only 11 pools across a much larger extent. Counts of the actual number of pools present at Otay Mesa were extracted from a GIS data set of pool identification numbers maintained the City, while those at Marron Valley were provided by Conservation Biology Institute. The extents of the Otay Mesa and Marron Valley sites utilized in this analysis are shown in Figure 2 and Figure 3, respectively.

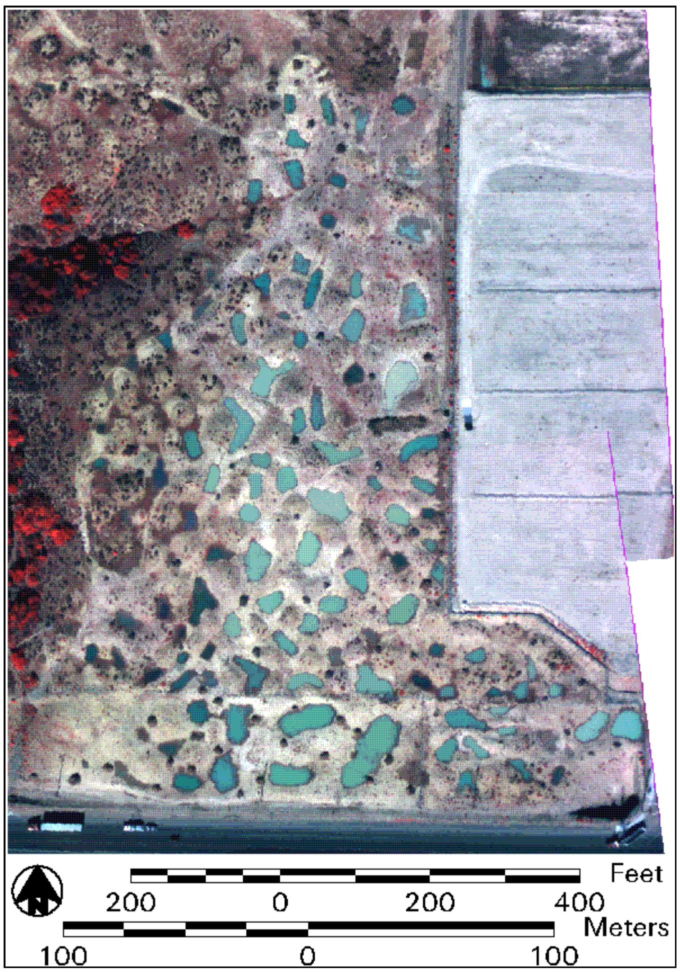

Figure 2. One foot ADAR imagery with pools interpreted at Otay Mesa. Display is color infrared (4,3,2).

An experiment was conducted in which nine interpreters visually identified apparent vernal pools beginning with the lowest resolution imagery and then with progressively higher spatial resolution imagery. The interpreters were first provided with training information on the characteristics of the vernal pools (size range, color, potential presence of vegetation at edge, etc.) and with graphic examples of vernal pools at the Otay Mesa site that were not included in the experiment. The interpretation experiment was carried out while viewing the imagery in digital format on computer monitors. During the experiment, interpreters used computer drawing tools to place an ellipse atop features they believed to be vernal pools. Once they completed interpretation of the 16 ft resolution imagery, they moved on to the 8 ft resolution imagery and started the interpretation over again creating a new drawing layer each time. In all, ninety interpretations were completed (2 sites x 5 resolutions x 9 interpreters). The number of pools correctly identified and the number of pools falsely identified were tallied up and analyzed in order to determine the optimum spatial resolution.

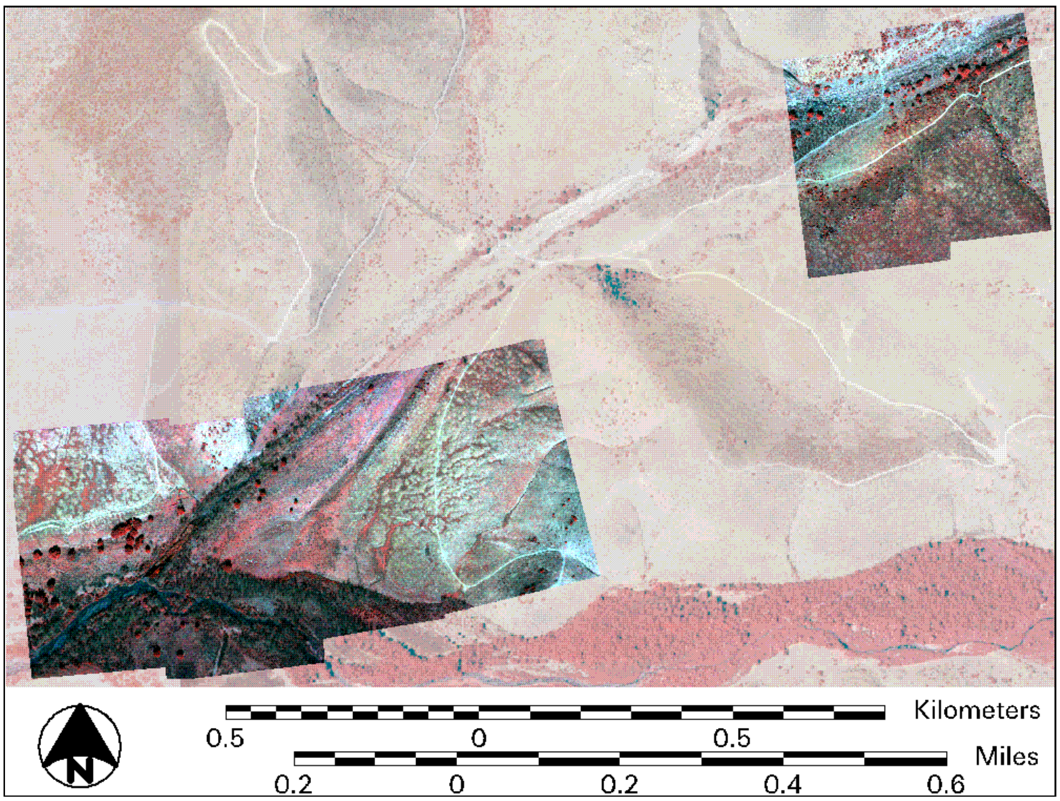

Figure 3. One foot ADAR imagery with pools interpreted at Marron Valley. The ADAR imagery is shown with a 2000 color-infrared orthophotograph as a backdrop. Display is color infrared (4,3,2).

The project team explored multiple methods of simulating low resolution imagery from imagery acquired at higher resolution. A simple aggregation of a large number of high spatial resolution pixels into a single lower resolution pixel does not adequately simulate imagery acquired at the lower spatial resolution. This is the case, because simple aggregation does not take into account the effects of atmospheric scattering nor path radiance introduced from adjacent pixels when acquiring lower resolution imagery from higher altitudes. Methods for accurately simulating lower resolution imagery from high resolution imagery were tested using archived ADAR 5500 data sets acquired at multiple resolutions as reference. The best method utilized a sequence of processing steps, where a low pass averaging filter was passes over the image and then the imagery was aggregated by a factor of two. This processing flow was carried out each time the image resolution was aggregated by a factor of two. Through the process, the size of the low pass filter (and therefore the averaging performed) varied between levels of aggregation, based upon operator judgment.

The complete processing flow utilized to generate the multiple resolution image sets at both Otay Mesa and Marron Valley sites is described as follows: 1) aggregate 1 ft image mosaic by a factor of 2 to generate the 2 ft mosaic; 2) run 3x3 low pass over 2 ft mosaic then aggregate resulting image by a factor of 2 to generate the 4 ft resolution mosaic; 3) run 5x5 low pass filter over 4 ft mosaic then aggregate resulting image by a factor of 2 to generate the 8 ft resolution mosaic; 4) run 3x3 low pass filter over 8 ft mosaic then aggregate by a factor of 2 to generate the 16 ft resolution image. The seemingly logical use of a 7x7 low pass filter in step #4 was found to overly smooth the resulting image. It was determined that the use of the 3x3 low pass filter in step #4 provided the best result.

4.2 Pool Vegetation Classification

The utility of ADAR 5500 imagery for discriminating individual plant species and classifying them using through semi-automated image classification was assessed with imagery acquired at 2 inch spatial resolution on May 23rd. This data set had very high resolution, providing the maximum detail for resolving individual plants and assemblages of homogenous cover (Figure 4). Prior to analysis, the normalized difference vegetation index (NDVI) was calculated using Equation 1 and was added as a fifth layer to the multispectral ADAR 5500 image mosaic. Spectral signatures were extracted and evaluated.

$$(\text{Near-infrared} - \text{Red}) \;/\; (\text{Near-infrared} + \text{Red}) \qquad \text{(Equation 1)}$$

The 2 inch resolution imagery was classified through unsupervised and supervised classification to test the utility of each. The imagery was first processed through unsupervised classification. For this classification, the 2 inch image mosaic was masked so that only image cells containing vegetation within the vernal pools were maintained for further analysis. This significantly reduced the variance within the data set and enabled the spectral clustering routine the maximum potential for discriminating the various types of plants within the pools. The masking was performed by first digitizing polygons around the pools and setting all data outside of the pools to zero (background). Following this step, non-vegetated portions of the image were masked and set to zero based upon a operator determined NDVI value below which ground cover no longer contained vegetation. This minimum NDVI value was determined to be 0.06.

Thirty spectral cluster classes were automatically generated by an ISODATA image processing routine. The spectral cluster classes were examined one at a time, compared to the reference data, and labeled with the class that they corresponded to in the reference data. While the reference data utilized to label spectral clusters was not independent of the validation data set, this approach provided the most exhaustive analysis of the spectral information content within

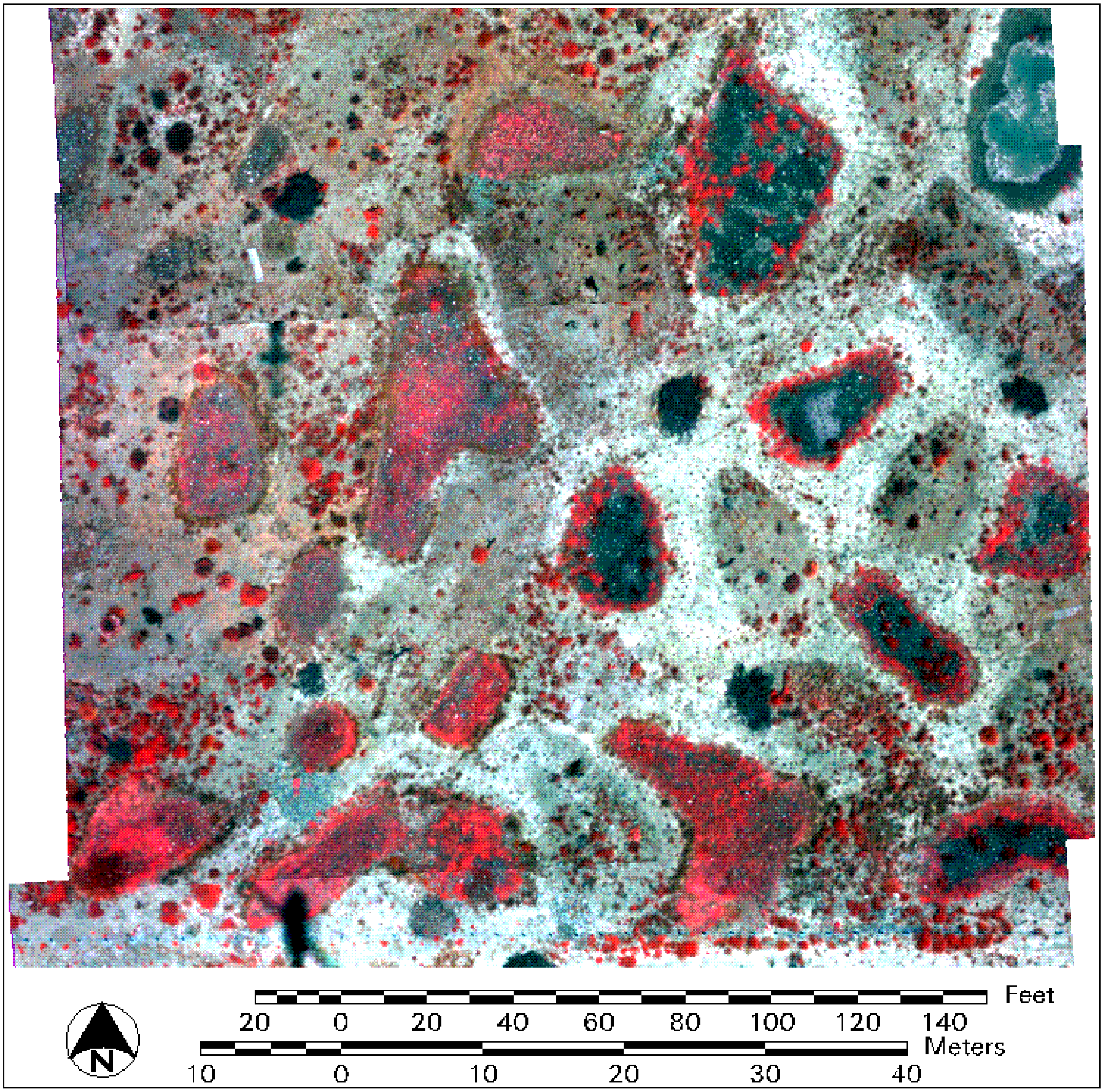

Figure 4. Selected portion of the May 23, 2001 2 inch resolution ADAR 5500 image mosaic. Display is color infrared (4,3,2).

the imagery. Five spectral cluster classes were found to be mixtures of two or more vegetation types. Pixels corresponding to these five classes were re-classified through an unsupervised classification cluster-busting approach. The refined classes were labeled and merged with the successfully labeled classes from the original unsupervised classification.

For the supervised classification, spectral signatures were extracted from the image mosaic, using the reference vegetation map as a guide. Fifty five signatures were extracted from the following classes Erar, Ponu, Elma, Psbr and Plagiobothrys acanthocarpus (Plac). Each of the fifty five signatures were extracted using multiple pixels from individual plants. Image classifications were generated using two signature set variations. For the first signature set, signatures of like plant types were aggregated on a pool by pool basis, resulting in seventeen signature sets. This design enabled the signatures to characterize the unique spectral response and background characteristics of plants within the individual pools sampled. For the second signature set, all signatures were aggregated by plant type. A total of six signatures resulted, as Elma plants within the study area were found to have two distinct signatures. Therefore, two final signatures were maintained to characterize the unique spectral characteristics Elma.

The spectral separability of individual plant species included in the spectral signature sets was assessed using spectral signature plots, feature space class ellipse plots, and the transformed divergence measure of spectral separability. Following review of the separability measures, supervised image classifications were generated for the two levels of signature aggregation. The accuracy of the classifications was assessed through comparison against the reference vegetation map. Contingency matrices illustrating classification agreement and disagreement with the reference data set were generated for each classification product.

4.3 Pool Water Depth

The depth of water within vernal pool basins significantly affects the abundance and diversity of plants and invertebrates that pools may support in a given season. To determine if high spatial resolution multispectral imagery could be utilized to estimate pool depth, three indices were generated from the February imagery and compared to field collected depth measurements at the Otay Mesa site. The computed spectral indices were: 1) red/blue ratio; 2) blue/near-infrared ratio; and 3) the normalized difference vegetation index. Examples of these image products are given in Figure 5.

The red/blue index has traditionally been utilized to estimate water transparency (i.e., secchi disk depth) (Lathrop et al., 1991). At shallow depths found within vernal pools, the red/blue index may also be related to water depth, if the index value decreases with increasing depth as the subsurface soil reflects less of the longer wavelength red light relative to blue light. Similarly, the near-infrared/blue index was tested under the assumption that there is significantly greater absorption of the longer near-infrared wavelength relative to the shorter blue wavelength as water depth increases. Therefore, there may be a positive relationship between the blue/NIR index and water depth. The NDVI is commonly used for vegetation analysis. However, the NDVI will also decrease with increasing water cover, because of the relatively high absorption of NIR by water bodies.

Reference water depth values were recorded at fifty five points within thirty pools at Otay Mesa during the field visit on February 5th. Pool depth was measured using a weighted string that was dangled from a hand-held boom. One inch increments were indicated on the string and pool depths were measured to the half inch. Pool depths ranged from 1.5 to 8.5 inches. Values from the three spectral indices were extracted from the imagery at each of the fifty five pool depth sample locations. R-Squared values from simple linear regression models between image-derived values and pool depth values were generated.

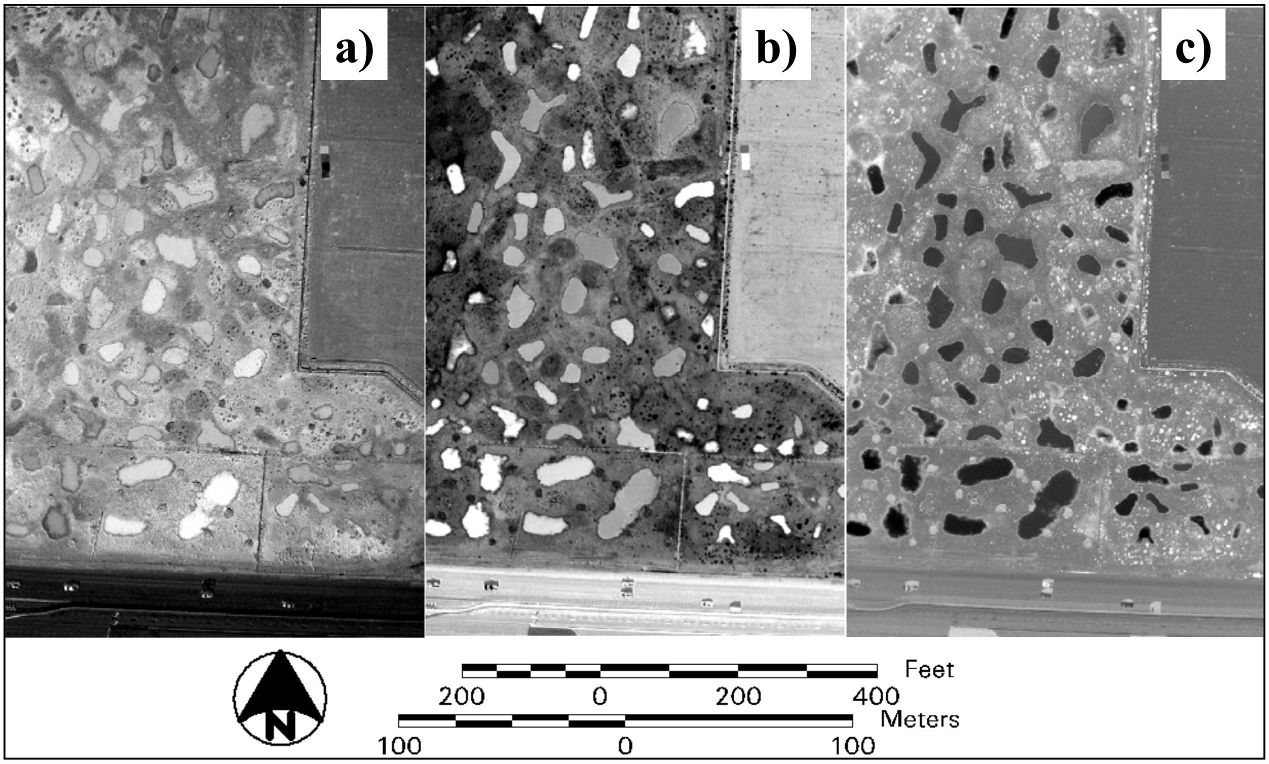

Figure 5. Spectral index products utilized during the pool water depth analysis. Image ratio products are: a) red/blue ratio; b) blue/near-infrared ratio; and c) normalized difference vegetation index.

4.4 Mapping Land Use and Land Cover Near Vernal Pools

The utility of high spatial resolution multispectral imagery for characterizing the condition of the landscape adjacent to vernal pools was qualitatively reviewed. The project sought to indicate the general utility of this imagery for mapping: 1) mima mound locations; 2) vernal pool watershed boundaries; 3) vegetation community type and level of disturbance; 4) land use adjacent to vernal pool sites (residential, agricultural, etc.); and 5) anthropogenic disturbances such as off-road vehicle activity.

5.0 Results and Discussion

5.1 Optimum Spatial Resolution for Pool Detection

Examples of vernal pools within the multiple resolution imagery simulated from 1 ft image mosaics at Otay Mesa and Marron Valley are illustrated in Figure 6. Interpretation accuracy generally improved as interpreters progressed from the 16 ft resolution imagery to the 2 ft resolution imagery. A slight reduction in accuracy occurred going from 2 ft to 1 ft resolution, as interpreters may have second guessed their interpretation of the 2 ft resolution imagery while interpreting the 1 ft resolution imagery. The number of pools correctly identified by each interpreter and summary statistics for the two study sites are given in Table 2. Plots of the average number of pools correctly interpreted per resolution are given in Figure 7 and Figure 8 for Otay Mesa and Marron Valley, respectively. Also shown on the plots are standard error bars (one standard deviation) illustrating the variability between the nine interpreters and a solid line indicating the total number of pools actually present at the sites. One hundred twenty five pools were located within the Otay Mesa image set and eleven pools were present within the Marron Valley image set.

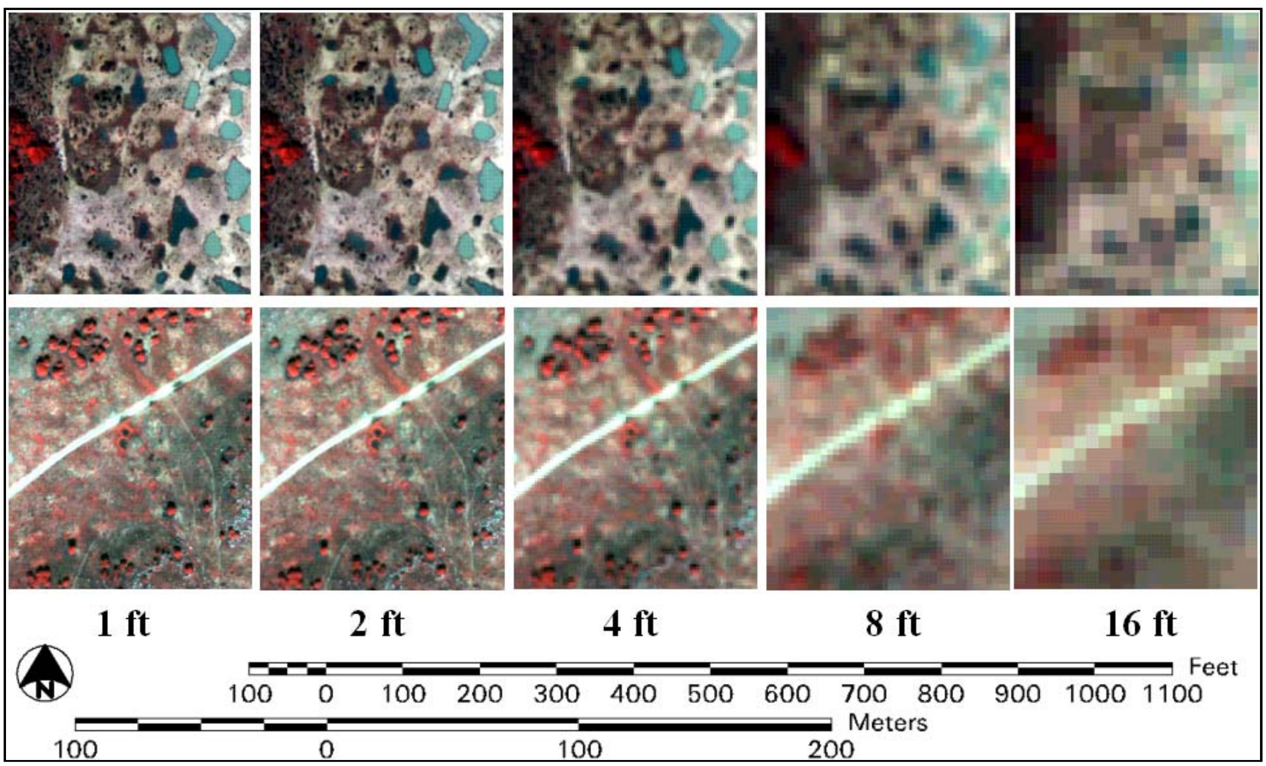

Figure 6. Vernal pools within multiple spatial resolution imagery at Otay Mesa (top) and Marron Valley (bottom).

Table 2. Number of pools correctly interpreted at Otay Mesa and Marron Valley sites. Total number of pools present is 125 at Otay Mesa and 11 at Marron Valley.

	Otay Mesa					Marron Valley				
Interpreter	**16 ft**	**8 ft**	**4 ft**	**2 ft**	**1 ft**	**16 ft**	**8 ft**	**4 ft**	**2 ft**	**1 ft**
1	6	34	79	101	90	1	2	4	4	3
2	37	88	87	92	90	1	0	6	7	4
3	41	85	102	112	111	0	3	7	6	7
4	0	56	81	99	93	0	0	5	5	5
5	51	64	93	95	95	0	1	3	5	5
6	68	82	92	102	105	0	0	1	7	7
7	27	69	92	93	98	2	2	5	7	6
8	4	88	100	100	105	2	6	10	7	6
9	5	86	41	99	102	0	5	10	4	5
Mean	26.6	72.4	85.2	99.2	98.8	0.7	2.1	5.7	5.8	5.3
Std. Dev.	24.3	18.5	18.3	6.0	7.4	0.9	2.2	3.0	1.3	1.3
Maximum	68	88	102	112	111	2	6	10	7	7
Minimum	0	34	41	92	90	0	0	1	4	3

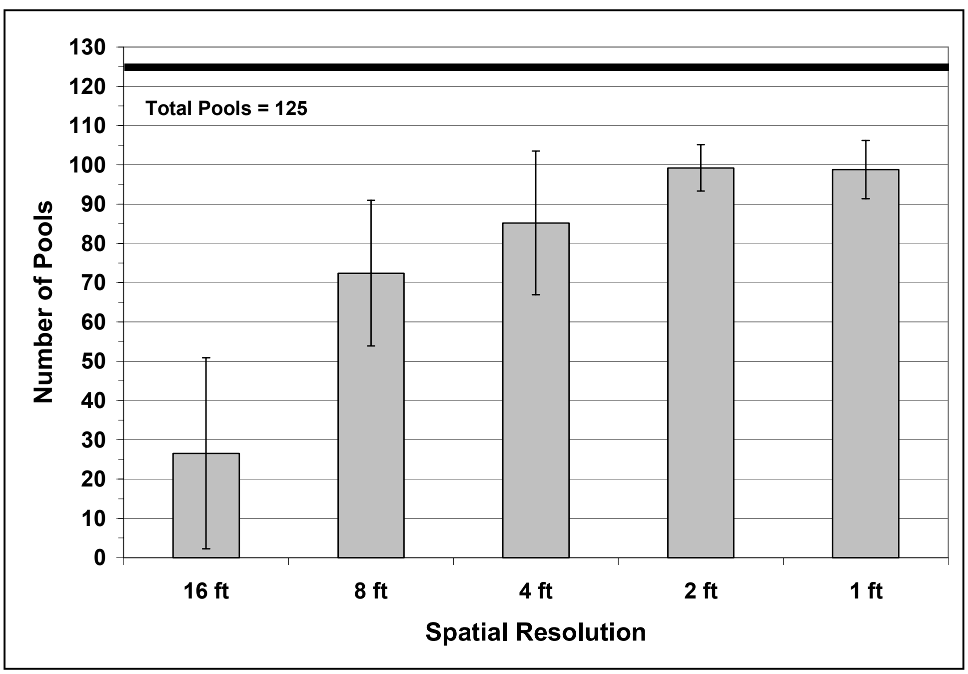

Figure 7. Average number of pools correctly interpreted at Otay Mesa site. Error bars represent variation between interpreters at one standard deviation. Total number of pools present is indicated by bold black line.

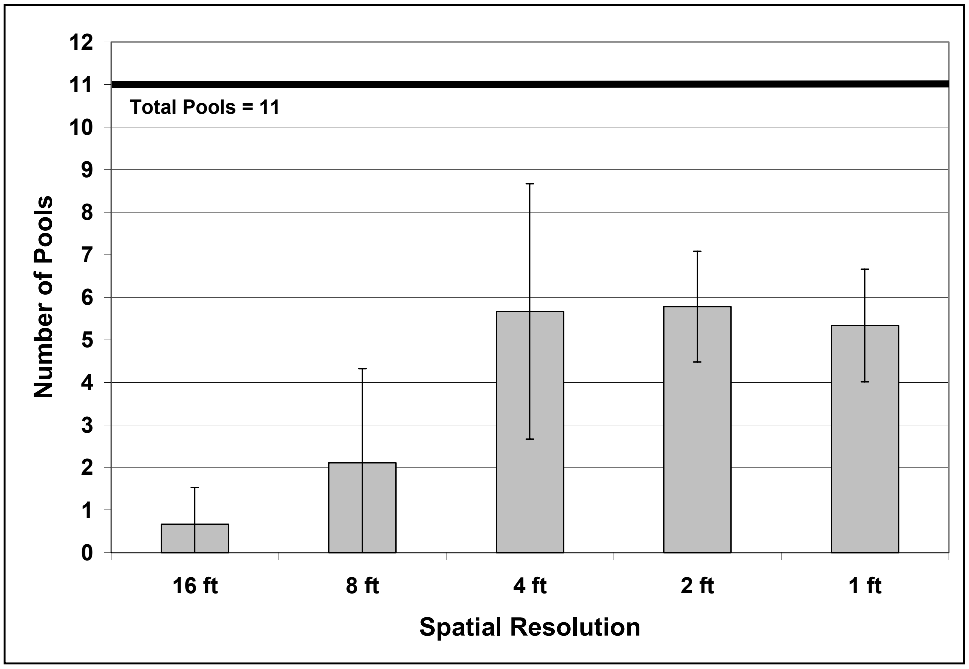

Figure 8. Average number of pools correctly interpreted at Marron Valley site. Error bars represent variation between interpreters at one standard deviation. Total number of pools present is indicated by bold black line.

The total number of falsely identified vernal pools was also compiled and summarized. These data and the associated summary statistics are given in Table 3. A greater number of pools were falsely identified at the Marron Valley site when compared to the Otay Mesa site. This is due to the relatively complex nature, dark color, and sparse presence of the natural pools at Marron Valley site.

Interpreters who had a few instances of extreme false identification are highlighted in Table 3. While interpreting the 4 ft resolution imagery at the Otay Mesa site, two interpreters confused dark patches of vegetation and/or brush piles as vernal pools. At the Marron Valley site, one interpreter, repeatedly confused dark, shaded areas as vernal pools and significantly overestimated the number of pools present. It is likely that interpreters with a greater understanding of vernal pools and more experience interpreting them would not falsely identify a great number of pools in this manner. If these extreme false identifications of vernal pools are excluded from the results, the number of false identifications is greatly reduced and the number of false identifications is relatively constant across all spatial resolutions interpreted. Figure 9 and Figure 10 illustrate the average number of false identifications per resolution at the Otay Mesa and Marron Valley sites, respectively, when the interpreters with extreme false identifications are not included. The variation between interpreters is indicated by the one standard deviation error bars.

Table 3. Number of pools falsely identified at Otay Mesa and Marron Valley sites. Extreme false interpretations indicated in gray are omitted from summary statistics.

	Otay Mesa					Marron Valley				
Interpreter	**16 ft**	**8 ft**	**4 ft**	**2 ft**	**1 ft**	**16 ft**	**8 ft**	**4 ft**	**2 ft**	**1 ft**
1	0	0	0	4	1	0	0	0	0	1
2	0	0	0	0	0	8	7	20	19	8
3	5	1	52	1	2	23	21	7	4	8
4	0	0	1	1	1	1	5	6	4	18
5	0	0	0	1	1	1	1	1	0	0
6	2	4	1	0	0	10	124	117	113	37
7	1	0	1	2	1	3	4	3	2	8
8	0	2	1	1	2	4	3	8	6	5
9	2	1	45	1	0	17	4	6	12	7
Mean	0.4	0.9	0.6	1.3	0.9	7.1	5.6	6.4	5.9	6.9
Std. Dev.	0.8	1.6	0.5	1.4	0.7	8.5	6.6	6.2	6.6	5.5
Maximum	2	4	1	4	2	23	21	20	19	18
Minimum	0	0	0	0	0	0	0	0	0	0

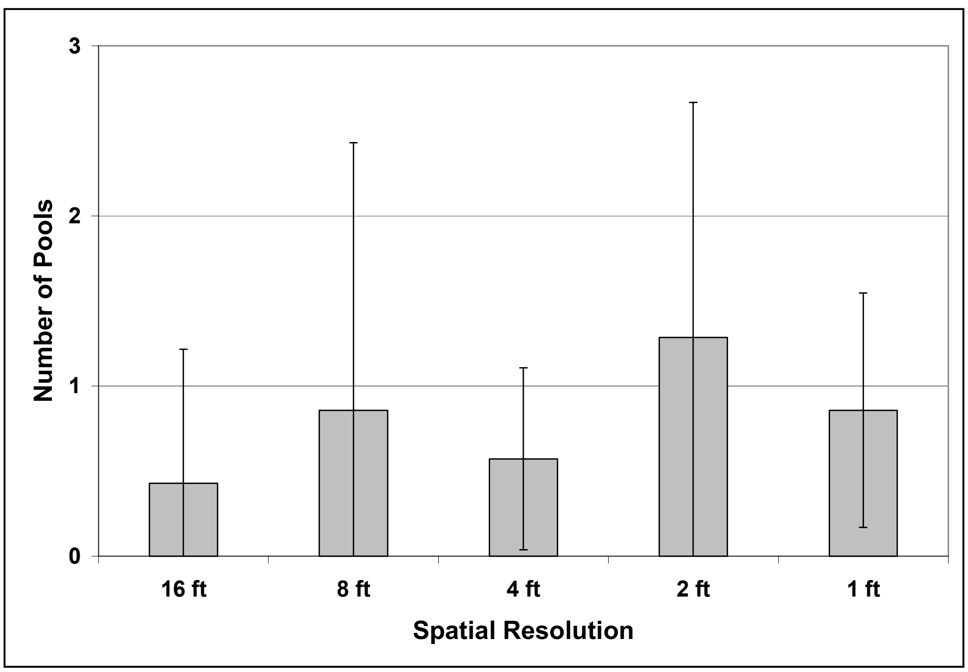

Figure 9. Average number of pools falsely interpreted at Otay Mesa site. Error bars represent variation between interpreters at one standard deviation. Extreme false interpretations are omitted from calculation of values.

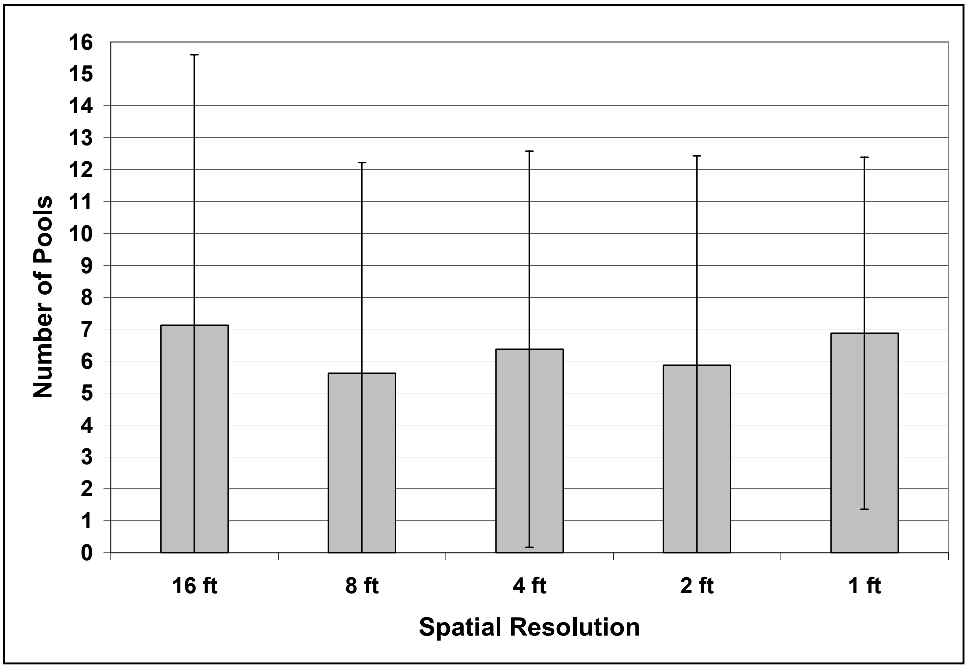

Figure 10. Average number of pools falsely interpreted at Marron Valley site. Error bars represent variation between interpreters at one standard deviation. Extreme false interpretations are omitted from calculation of values.

Results suggest that the optimum spatial resolution for detecting vernal pools within multispectral imagery is 2 ft. Approximately 80% of the pools at Otay Mesa and 55% of the pools at Marron Valley were accurately identified using the simulated 2 ft resolution imagery. At 4 ft spatial resolution, the average number of pools correctly identified was approximately 70% at Otay Mesa and 55% at Marron Valley. While the average number of pools correctly identified with 2 ft and 4 ft resolution imagery was nearly the same at Marron Valley, the variation between interpreters at the 4 ft resolution is double that of the 2 ft resolution, suggesting lower confidence with the 4 ft resolution imagery. The final decision on spatial resolution will be based upon a compromise between accuracy and cost. These results also suggest that the number of false identifications is not likely to be a function of image spatial resolution, as the number of false identifications is relatively constant between all spatial resolutions.

Accuracy may be expected to improve given interpreters with more experience with vernal pool characteristics and interpretation skills. In addition, spectral index products generated from high spatial resolution multispectral imagery may aide in the interpretation of the imagery. Products generated for the pool water depth analysis illustrate the utility of such enhancements (Figure 5).

The precision with which vernal pool basins may be delineated using multispectral imagery is a function of the spatial resolution of the imagery. Visual analysis of the wet season (February) imagery utilized in this project, in conjunction with field reconnaissance, suggest that the precision of pool basin delineation is on the order of +/- 1 to 2 pixels at the wet/water-filled edge of the pools. Therefore, vernal pools may be delineated through interpretation of 2 ft spatial resolution imagery with a precision of +/- 2 to 4 ft at these wet edges. When vernal pools are not filled, bare soil and/or vegetated rings around the pools may indicate the full extent of the basin. However, the accuracy with which perimeters of vernal pools may be delineated based upon pool edge characteristics is likely to vary by site. Review of 1 m panchromatic satellite imagery from a portion of Del Mar Mesa known to contain vernal pools demonstrates that even dry vernal pool basins may be detected and delineated if the reflectance of surrounding land cover is sufficiently different (Figure 11). Of course, the presence of water within the basins provides additional confidence in the interpretation, detection, and delineation of vernal pool basins

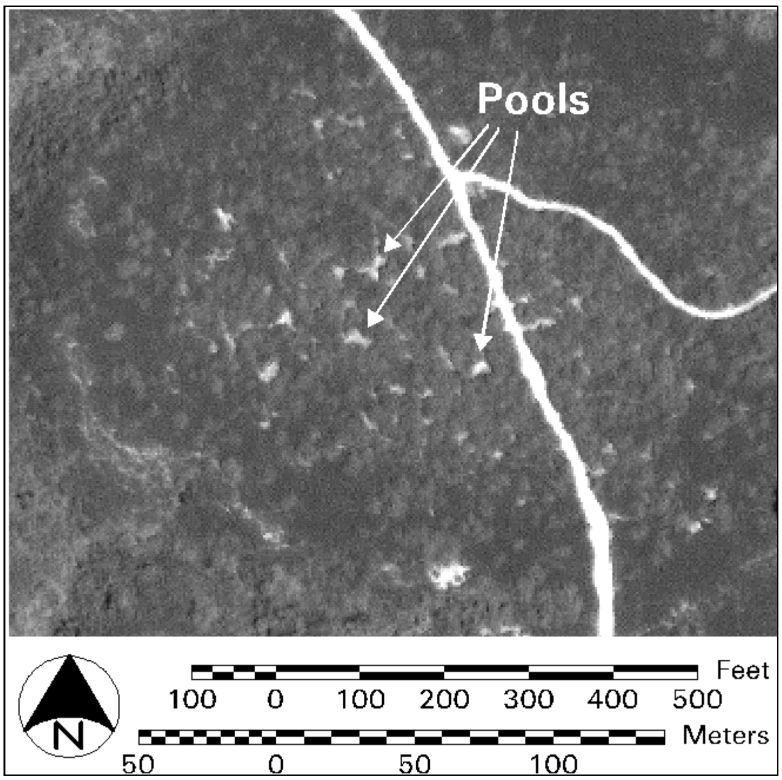

Figure 11. Dry vernal pools apparent in 1 m panchromatic IKONOS imagery at Del Mar Mesa.

This project sought to validate the delineation of vernal pool basins by using GIS data sets of basin perimeters which were provided by the City of San Diego and correspond to the City owned vernal pools at the Otay Mesa site. However, these data could not be utilized to validate image-derived basin perimeters because the GIS data was based-upon basin "as-built" construction plans and did not exactly correspond to the actual post-construction configuration of the pools. Figure 12 illustrates the spatial non-correspondence of the GIS data sets from the construction plan and the actual post-construction site conditions as documented in the 2000 color-infrared orthophoto product and the February 2001 ADAR image mosaic.

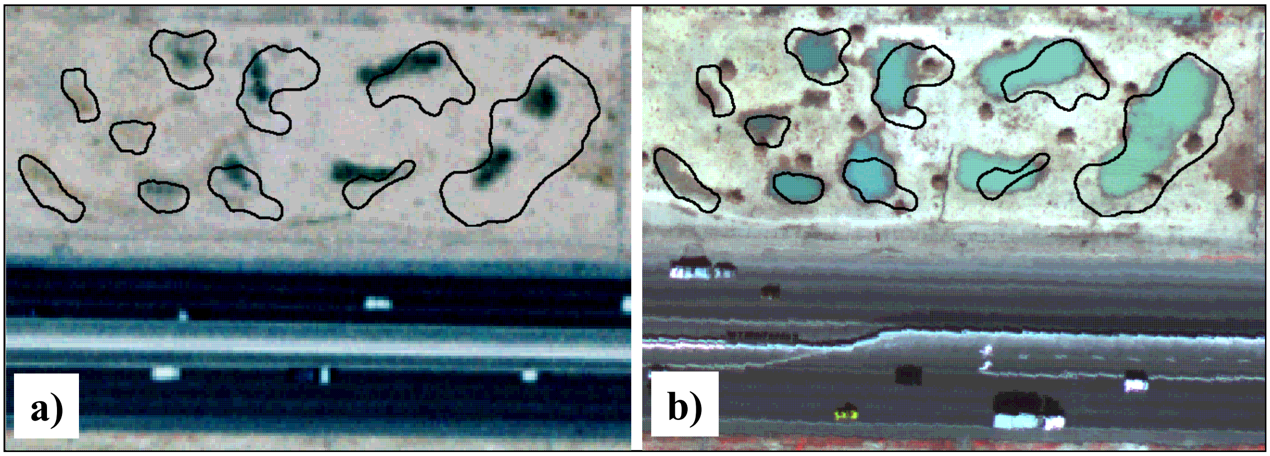

Figure 12. Spatial non-correspondence between imaged vernal pool conditions and "as-built" GIS layer of pool basin perimeters. Pool perimeter GIS layer is overlaid with: a) 2000 color-infrared 2 ft orthophotograph and b) 2001 ADAR 5500 1 ft imagery.

5.2 Pool Vegetation Classification

5.2.1 Unsupervised Classification

Six plant types were classified using the unsupervised classification approach. Many spectral clusters corresponded well with either the Erar or the Elma plants, as depicted on the reference map. Four spectral cluster classes were found to correspond well with areas mapped as Psbr, with little overlap with other potential plant types present on the reference map. These Psbr cluster classes were generally located as rings around the outside perimeter of the pools. Two spectral clusters corresponded well to a polygon of Ponu and to mixed polygons which were labeled as containing Ponu. However, no other cluster classes corresponded to polygons mapped as Ponu. One spectral cluster class corresponded to a polygon mapped as mixed that contained Jubu and did not correspond to any other plant type field mapped. This spectral cluster class was labeled as Jubu. One spectral cluster class was labeled as *Lilaea scilloides* (Lisc), as it corresponded most to a polygon mapped as Lisc and did not correspond to any other plant type mapped. However, only a small fraction of the Lisc polygon contained pixels from this spectral cluster class. Therefore, overall agreement for this class is expected to be low.

The mean of spectral cluster classes generated through unsupervised image classification are plotted as stars within the red (X-axis) and near-infrared (Y-axis) feature-space of the full (non-masked) 2 inch resolution ADAR mosaic in Figure 13. The white ellipses represent variation within the spectral cluster class at one standard deviation from the mean (68% of the data from these cluster classes lies within the ellipse). Elma plants are generally characterized as having low red and low near-infrared values. Erar plants are generally characterized as having mid-level red values and mid to high near-infrared values. Psbr plants demonstrated high red and high near-infrared values as the plants were scenescing and had exposed soil around them. Spectral cluster classes labeled as Ponu, Lisc, and Jubu had mid-range values in red and NIR.

Spectral signatures from the unsupervised classification spectral cluster classes are shown in Figure 14. The five plant types generally show a range of brightness values in the blue, green, and red (visible) wavebands. Spectral distinctions between the vegetation types are primarily indicated by differences in the red, near-infrared, and NDVI layers (layers 3,4, and 5).

Results from the accuracy assessment of the unsupervised classification are given in Table 4. Results are given for producer's accuracy, user's accuracy, and overall accuracy. Results are expressed in terms of pixel counts (number of 2 inch resolution pixels) and in terms of percentage of class for both the producer's and user's accuracy. Producer's accuracy indicates errors of omission and is calculated by dividing the number of pixels accurately classified into a given class by the number of pixels actually belonging to that class (as indicated by the reference map). User's accuracy indicates errors of commission and is calculated by dividing the number of pixels accurately classified into a given class by the total number of pixels classified into that class. Overall accuracy relates to all classes and is calculated as the total number of pixels accurately classified divided by the total number of pixels classified. Overall accuracy is biased by classes having a large number of pixels relative to the other classes.

The overall accuracy of the unsupervised classification was 68.53%. However, this accuracy is biased by the Erar and Elma classes, as they classified with relatively high accuracy and represented approximately 86.5% of the total area mapped. The producer's accuracy for Erar and Elma were 72.31% and 74.48%, respectively. Producer's accuracy for Ponu, Psbr, and Lisc were relatively low, as much of what was field mapped as these classes, was classified as Erar. Plac did not correspond to any spectral cluster classes and was not classified in the unsupervised classification.

Measures of user's accuracy from the unsupervised classification indicate that Erar was not significantly over-classified, as 86.28% of what was classified as Erar actually corresponded to Erar in the reference map. Elma was slightly over-classified, as 28.97% of what was classified as Elma was actually Erar on the reference map. Ponu was over-classified, as 65.16% of pixels classified as Ponu corresponded to Erar on the reference map and 26.72% of what was classified as Ponu corresponded to Elma on the reference map. Lisc was similarly over-classified as many pixels classified as Lisc corresponded to Erar and Elma on the reference map. Much of what was classified as Psbr also corresponded to Erar on the reference map. While the user's accuracy measures indicate confusion between classes, the percentage values are significantly influenced by the relatively large area of Erar and Elma classes present in the reference map, compared to the area of the Ponu, Psbr, and Lisc classes.

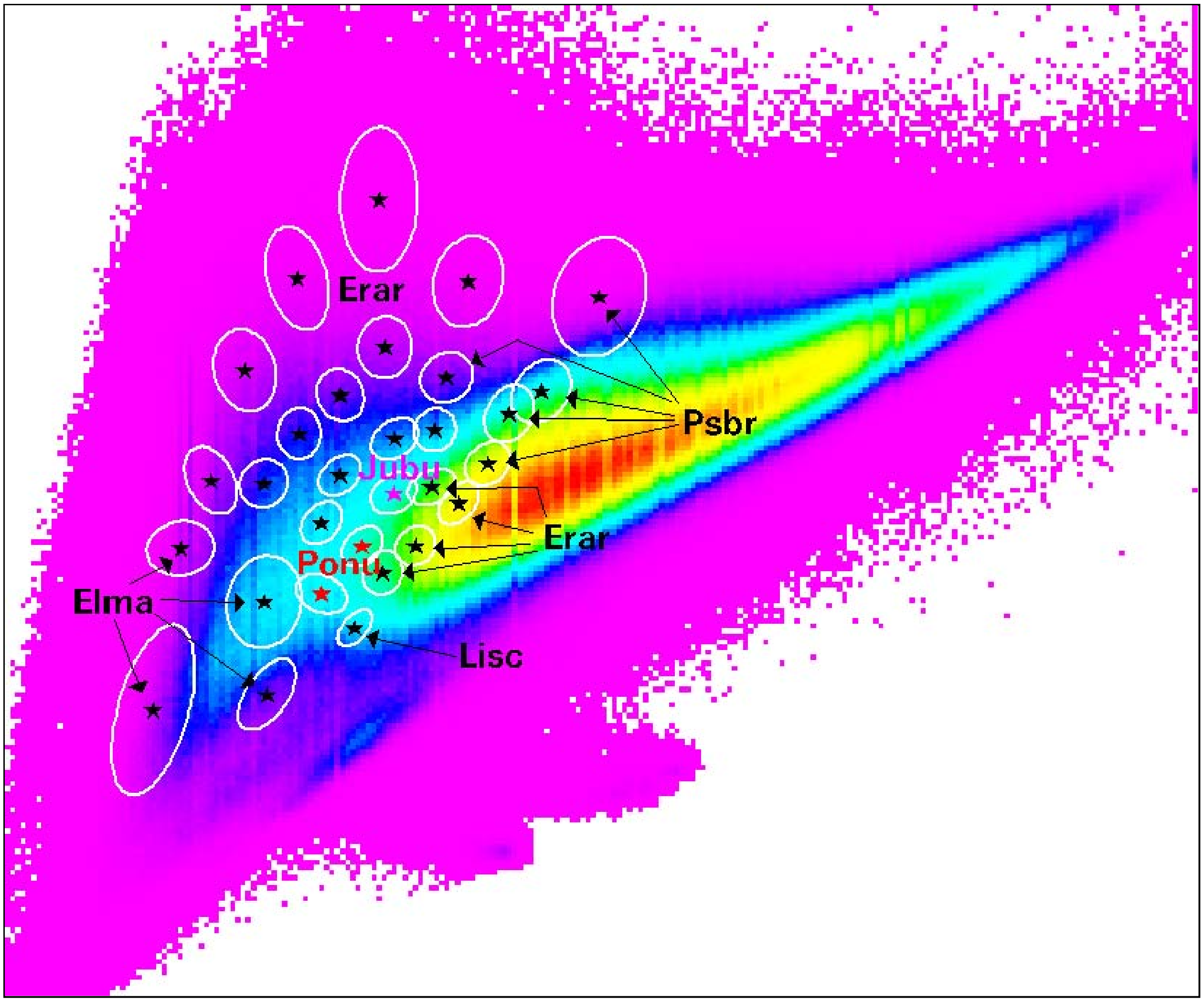

Figure 13. Unsupervised classification spectral cluster classes plotted within the red (X-axis) and near-infrared (Y-axis) feature-space. Stars represent class means, while the white ellipses represent variation within the spectral cluster class at one standard deviation from the mean.

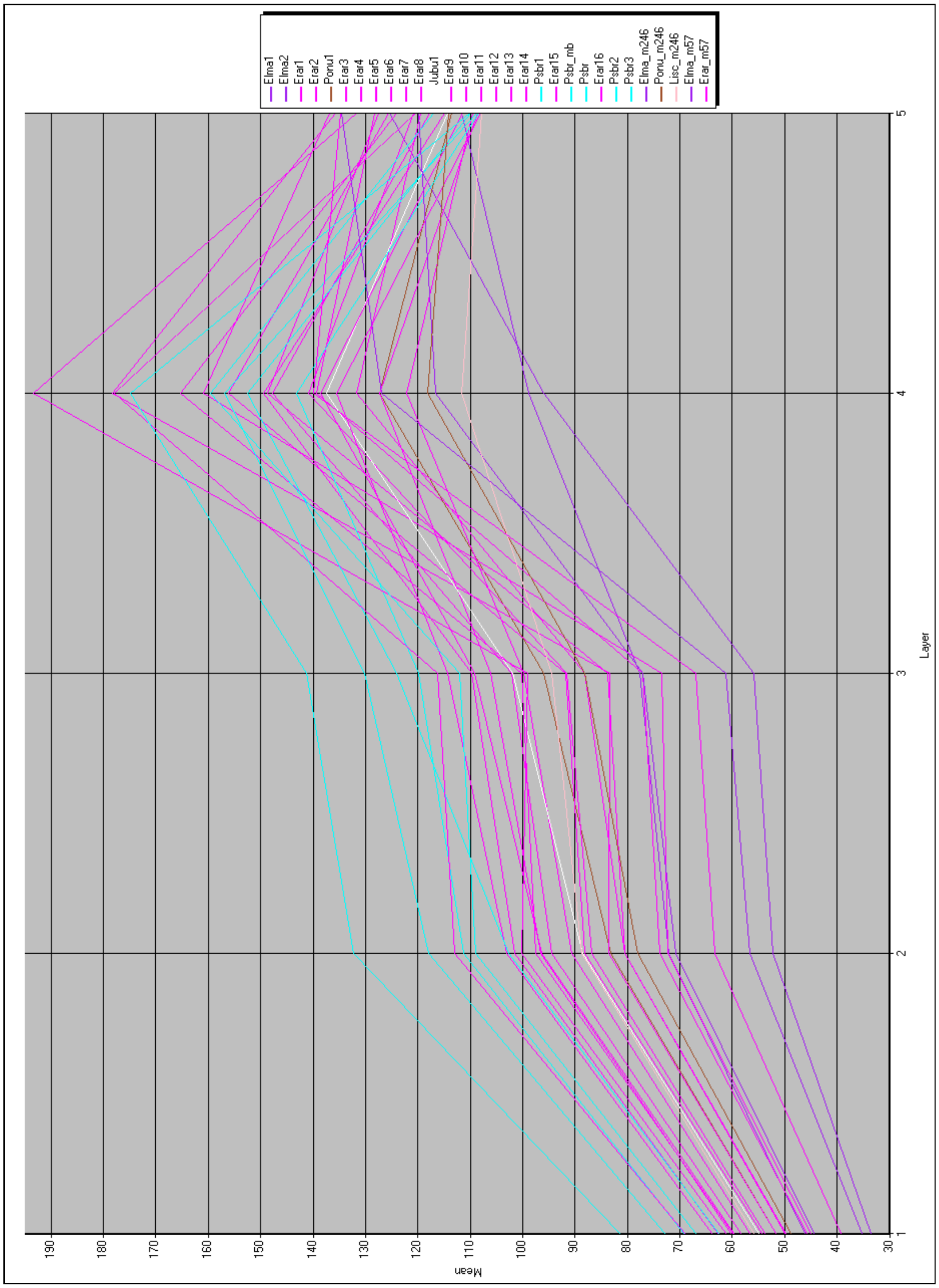

Figure 14. Spectral signatures of spectral cluster classes from unsupervised classification. NDVI is represented as layer 5.

Table 4. Accuracy assessment for the unsupervised classification.

Producer's Accuracy (Errors of Omission)

Classification	Reference Map						
	Erar	**Ponu**	**Elma**	**Jubu**	**Psbr**	**Lisc**	**Plac**
Erar	**140411**	1566	8045	0	11622	798	288
Ponu	7739	**163**	3173	0	164	121	517
Elma	15385	432	**36125**	0	225	8	929
Jubu	4860	57	355	**0**	134	33	15
Psbr	24948	458	325	0	**5237**	23	14
Lisc	843	79	481	0	4	**237**	32
Plac	0	0	0	0	0	0	**0**

Classification	Reference Map						
	Erar	**Ponu**	**Elma**	**Jubu**	**Psbr**	**Lisc**	**Plac**
Erar	**72.31%**	56.84%	16.59%	0.00%	66.85%	65.41%	16.04%
Ponu	3.99%	**5.92%**	6.54%	0.00%	0.94%	9.92%	28.80%
Elma	7.92%	15.68%	**74.48%**	0.00%	1.29%	0.66%	51.75%
Jubu	2.50%	2.07%	0.73%	**0.00%**	0.77%	2.70%	0.84%
Psbr	12.85%	16.62%	0.67%	0.00%	**30.12%**	1.89%	0.78%
Lisc	0.43%	2.87%	0.99%	0.00%	0.02%	**19.43%**	1.78%
Plac	0.00%	0.00%	0.00%	0.00%	0.00%	0.00%	**0.00%**

User's Accuracy (Errors of Commission)

Reference Map	Classification						
	Erar	**Ponu**	**Elma**	**Jubu**	**Psbr**	**Lisc**	**Plac**
Erar	**140411**	7739	15385	4860	24948	843	0
Ponu	1566	**163**	432	57	458	79	0
Elma	8045	3173	**36125**	355	325	481	0
Jubu	0	0	0	**0**	0	0	0
Psbr	11622	164	225	134	**5237**	4	0
Lisc	798	121	8	33	23	**237**	0
Plac	288	517	929	15	14	32	**0**

Reference Map	Classification						
	Erar	**Ponu**	**Elma**	**Jubu**	**Psbr**	**Lisc**	**Plac**
Erar	**86.28%**	65.16%	28.97%	89.11%	80.46%	50.30%	0.00%
Ponu	0.96%	**1.37%**	0.81%	1.05%	1.48%	4.71%	0.00%
Elma	4.94%	26.72%	**68.03%**	6.51%	1.05%	28.70%	0.00%
Jubu	0.00%	0.00%	0.00%	**0.00%**	0.00%	0.00%	0.00%
Psbr	7.14%	1.38%	0.42%	2.46%	**16.89%**	0.24%	0.00%
Lisc	0.49%	1.02%	0.02%	0.61%	0.07%	**14.14%**	0.00%
Plac	0.18%	4.35%	1.75%	0.28%	0.05%	1.91%	**0.00%**

Overall Accuracy: 68.53%

5.2.2 Supervised Classification, First Signature Set

The first supervised classification utilized multiple spectral signatures which were derived by aggregating signatures of like plant types on a pool by pool basis. A total of seventeen signatures from Erar, Ponu, Elma, Psbr, and Plac plant types were utilized. Signature means are plotted as stars within the red (X-axis) and near-infrared (Y-axis) feature-space of the full (non-masked) 2 inch resolution mosaic in Figure 15. The white ellipses represent variation within the signatures at two standard deviations from the mean (95% of the data from these signatures lies within the ellipse). Erar signatures are generally clustered with high values in the near-infrared. Most Elma signatures are clustered with low red and low near-infrared values. However, one Elma signature derived from plants that were largely submerged within a pool has a low NIR and a higher red value, relative to the other Elma signatures. Figure 15 illustrates that Erar signatures overlap with Elma and Psbr, and that Elma, Ponu, and Plac signatures overlap. Spectral signatures across all 5 layers (blue, green, red, NIR, and NDVI) are illustrated in Figure 16. It is clear that within-class signatures from the first supervised classification are more homogenous than signatures from the unsupervised classification spectral cluster classes. It is also clear that the Ponu signature is very similar to one of the Plac signatures, indicating that they are likely to be confused in the classification.

Accuracy assessment results for the first supervised classification are given in Table 5. The overall accuracy is 65.54%. Erar accuracy did not change, relative to accuracy associated with the unsupervised classification. Ponu classified better through supervised classification, as the producer's accuracy increased from 5.92% to 14.34%. Producer's accuracy for the Elma class decreased, as inclusion of Plac into the classification resulted in 23.71% of what is Elma in the reference to be classified as Plac in the supervised classification. However, the user's accuracy indicates that 67.67% of what was classified as Elma actually corresponds to Elma in the reference (similar to the unsupervised classification results). Psbr producer's accuracy slightly improved between the unsupervised and the first supervised classification. However, Psbr was also over-classified, as 77.33% of what was classified as Psbr corresponds to Erar on the reference map. Lisc was not included in the supervised classification, because field delineation of the reference polygon was imprecise and there was no clear indication of which plant cover in the polygon was Lisc. Therefore, accuracy for this class is zero in the supervised classification. The small area mapped as Plac was classified with 67.24% producer's accuracy. However, the user's accuracy indicates that Plac was significantly over-classified, as only 4.66% of what was classified as Plac actually corresponds to Plac on the reference map. Most of the area classified as Plac corresponds to Erar and Elma on the reference map.

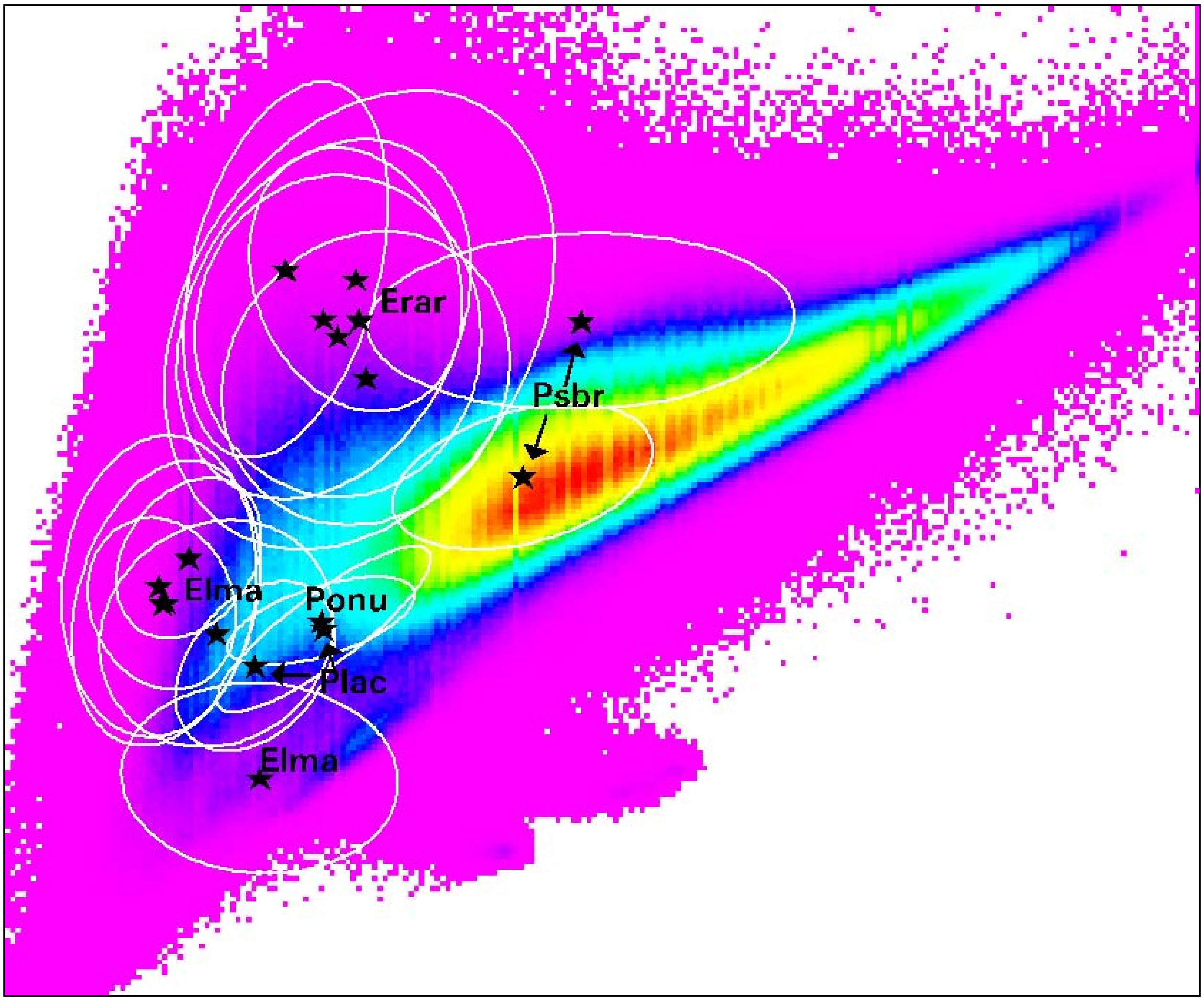

Figure 15. Plant signatures from the first supervised classification signature set plotted within the red (X-axis) and near-infrared (Y-axis) feature space. Signatures of like plant types were aggregated on a pool by pool basis. Stars represent signature means, while the white ellipses represent variation within the spectral signature at two standard deviations from the mean.

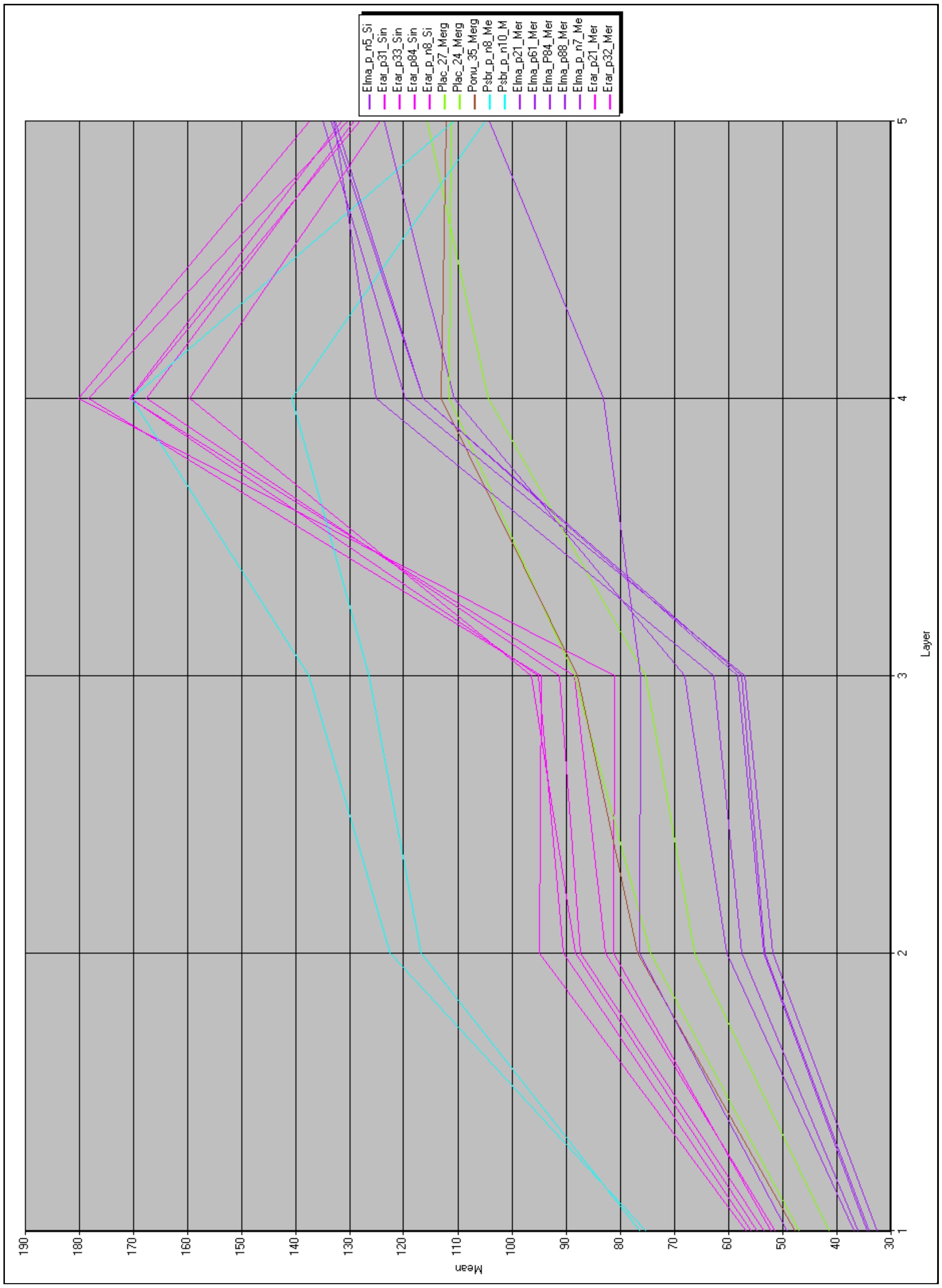

Figure 16. Spectral signatures from the first supervised classification signature set. Signatures of like plant types were aggregated on a pool by pool basis. NDVI is represented as layer 5.

Table 5. Accuracy assessment for the first supervised classification signature set. Signatures of like plant types were aggregated on a pool by pool basis.

Producer's Accuracy (Errors of Omission)

Classification — *Reference Map*

	Erar	Ponu	Elma	Jubu	Psbr	Lisc	Plac
Erar	**138398**	1378	6095	0	10321	153	58
Ponu	4358	**395**	2684	0	54	612	335
Elma	12420	374	**27678**	0	285	5	141
Jubu	0	0	0	**0**	0	0	0
Psbr	26427	356	549	0	**6545**	243	54
Lisc	0	0	0	0	0	**0**	0
Plac	12583	252	11498	0	181	207	**1207**

Classification — *Reference Map*

	Erar	Ponu	Elma	Jubu	Psbr	Lisc	Plac
Erar	**71.27%**	50.02%	12.57%	0.00%	59.36%	12.54%	3.23%
Ponu	2.24%	**14.34%**	5.53%	0.00%	0.31%	50.16%	18.66%
Elma	6.40%	13.58%	**57.06%**	0.00%	1.64%	0.41%	7.86%
Jubu	0.00%	0.00%	0.00%	**0.00%**	0.00%	0.00%	0.00%
Psbr	13.61%	12.92%	1.13%	0.00%	**37.65%**	19.92%	3.01%
Lisc	0.00%	0.00%	0.00%	0.00%	0.00%	**0.00%**	0.00%
Plac	6.48%	9.15%	23.71%	0.00%	1.04%	16.97%	**67.24%**

User's Accuracy (Errors of Commission)

Reference Map — *Classification*

	Erar	Ponu	Elma	Jubu	Psbr	Lisc	Plac
Erar	**138398**	4358	12420	0	26427	0	12583
Ponu	1378	**395**	374	0	356	0	252
Elma	6095	2684	**27678**	0	549	0	11498
Jubu	0	0	0	**0**	0	0	0
Psbr	10321	54	285	0	**6545**	0	181
Lisc	153	612	5	0	243	**0**	207
Plac	58	335	141	0	54	0	**1207**

Reference Map — *Classification*

	Erar	Ponu	Elma	Jubu	Psbr	Lisc	Plac
Erar	**88.49%**	51.65%	30.36%	0.00%	77.33%	0.00%	48.53%
Ponu	0.88%	**4.68%**	0.91%	0.00%	1.04%	0.00%	0.97%
Elma	3.90%	31.81%	**67.67%**	0.00%	1.61%	0.00%	44.35%
Jubu	0.00%	0.00%	0.00%	**0.00%**	0.00%	0.00%	0.00%
Psbr	6.60%	0.64%	0.70%	0.00%	**19.15%**	0.00%	0.70%
Lisc	0.10%	7.25%	0.01%	0.00%	0.71%	**0.00%**	0.80%
Plac	0.04%	3.97%	0.34%	0.00%	0.16%	0.00%	**4.66%**

Overall Accuracy: 65.54%

5.2.3 Supervised Classification, Second Signature Set

The second supervised classification utilized spectral signatures derived by aggregating all signatures by plant type. Two signatures were maintained for the Elma class to represent non-submerged and submerged conditions. A total of six signatures from Erar, Ponu, Elma, Psbr, and Plac plant types were utilized. Signature means are plotted as stars within the red (X-axis) and near-infrared (Y-axis) feature-space of the full (non-masked) 2 inch resolution mosaic in Figure 17. The white ellipses represent variation within the signatures at two standard deviations from the mean (95% of the data from these signatures lies within the ellipse). As with the first supervised classification, it is clear from Figure 17 that there is spectral overlap between Erar and Psbr signatures and between Elma, Ponu, and Plac signatures. Spectral signatures across all five layers (blue, green, red, NIR, and NDVI) are illustrated in Figure 18. Most classes demonstrate distinct spectral signatures. However, the Ponu and Plac signatures are very similar, suggesting that these plant types are not likely to be discriminated.

Accuracy assessment results for the second supervised classification are given in Table 6. The overall accuracy is 61.47%. Erar producer's accuracy decreased as Plac was over-classified and 17.94% of what is Erar was classified as Plac. Producer's accuracy for Ponu increased from 14.34% to 17.68% between the first and second supervised classification. However, Ponu continued to be over-classified, as the User's accuracy is 4.49%. There was little difference in the classification of Elma and Psbr between the first and second supervised classifications. Plac producer's accuracy decreased from 67.24% to 60.39%, as an increasing amount of what was mapped as Plac on the reference was classified as Ponu.

5.2.4 Image Classification Discussion

The unsupervised image classification had the highest overall accuracy at 68.53%. The accuracy of the first and second classifications were 65.54% and 61.47%, respectively. Erar and Elma plants classified with the highest accuracy had the highest user's and producers accuracy in the unsupervised classification. Producer's accuracy was 72.31% and 74.48% for Erar and Elma, respectively, in the unsupervised classification. This indicates that approximately 75% of the areas field mapped as Erar and Elma were classified correctly.

Ponu and Psbr classification accuracy was higher using supervised image classifications. However, each of these two plant types demonstrated significant spectral confusion with Erar and their classification accuracy was still low. Psbr accuracy was around 40% and Ponu accuracy was around 15%. Ponu represented less than 2% of the total area mapped as reference and may have been classified with higher accuracy if there were more sample sites for signature extraction. Further, polygons delineating Ponu on the hardcopy field maps were coarse relative to the small plants, and only 25-50% of the cover in the delineated polygons actually contained Ponu. It is likely that the classification accuracy of Ponu would be greater given additional training sites and with better reference data containing units of homogenous cover.

Analysis of the utility of image classification for identifying Lisc was confounded by having only one reference polygon with heterogeneous cover and no distinct delineation of the Lisc plants within the polygon. One spectral cluster in the unsupervised classification corresponded with the Lisc reference polygon and was classified with a producer's accuracy of almost 20%. However, this could be in error. There was no obvious plant within that field mapped polygon from which to take a signature for supervised classification. Further, this single polygon represented less than 1% of the reference classes mapped. Future studies are required if conclusions are to be drawn regarding image classification of this plant type.

The few occurrences of Plac (less than 1% of the reference map) were classified with 60-70% producer's accuracy in the supervised classifications. However, user's accuracy was low, suggesting that Plac was over-classified and reduced classification accuracy for Erar and Elma.

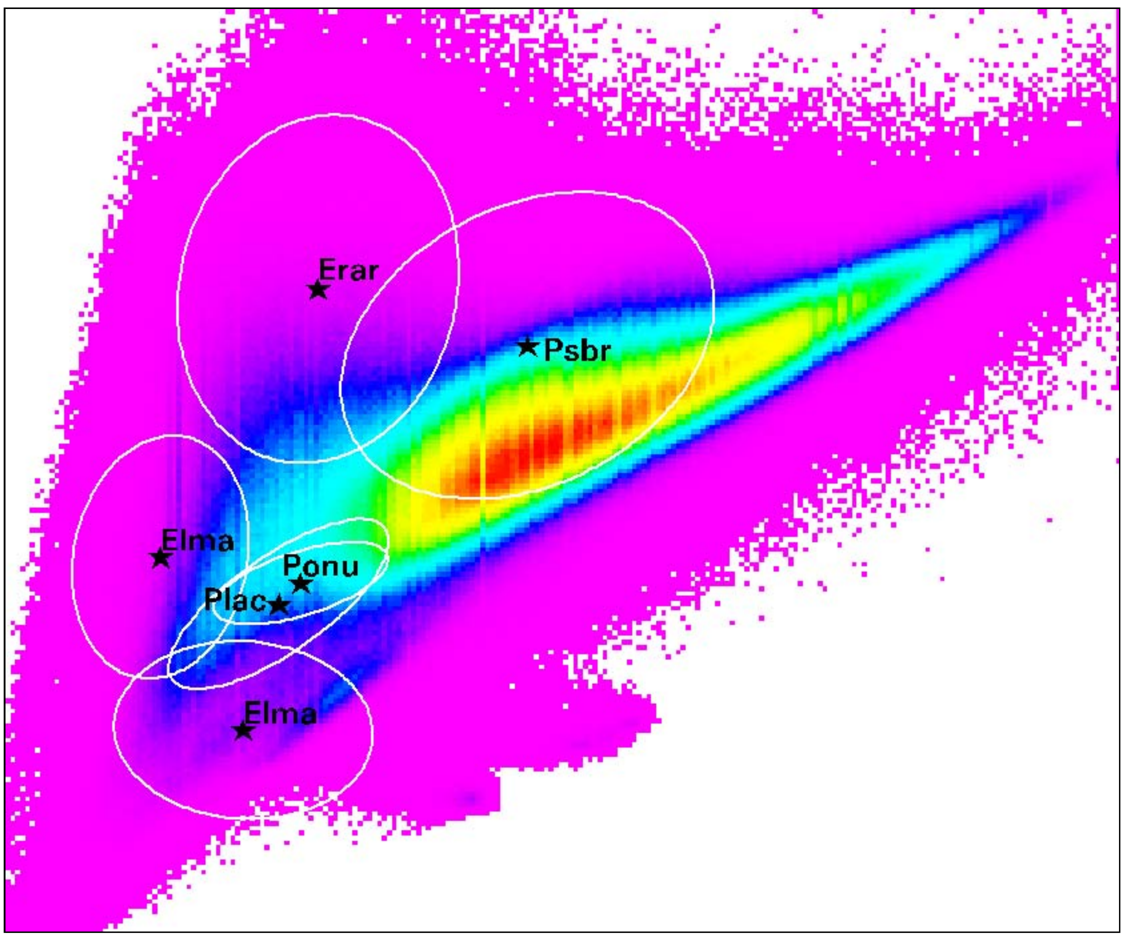

Figure 17. Plant signatures from the second supervised classification signature set plotted within the red (X-axis) and near-infrared (Y-axis) feature space. Signatures of like plant types were aggregated into a single signature. Elma plants had two distinct signatures representing submerged and non-submerged conditions. Stars represent signature means, while the white ellipses represent variation within the spectral signature at two standard deviations from the mean.

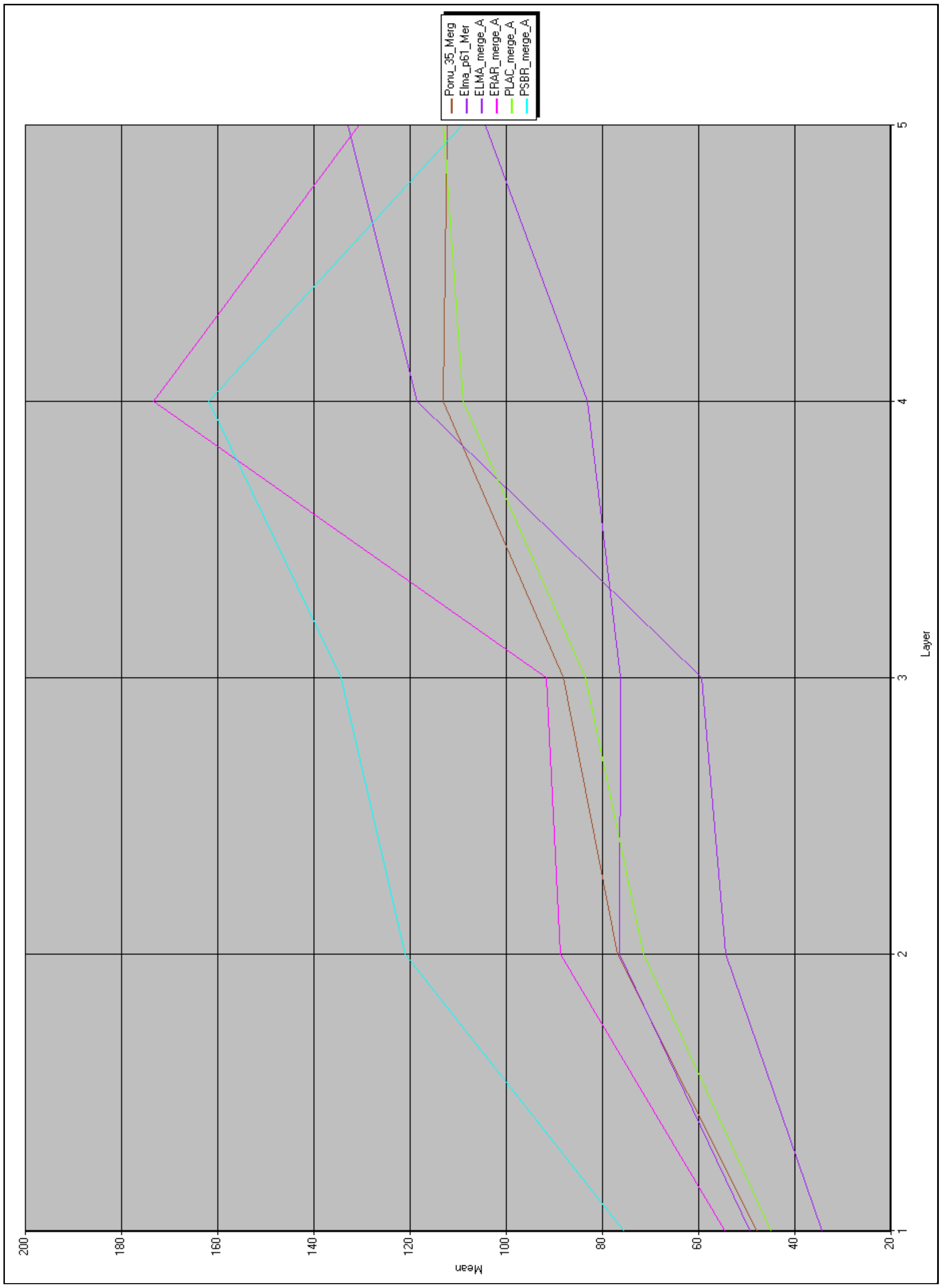

Figure 18. Spectral signatures from the second supervised classification signature set. Signatures of like plant types were aggregated into a single signature. Erar plants had two distinct signatures representing submerged and non-submerged conditions. NDVI is represented as layer 5.

Table 6. Accuracy assessment for the second supervised classification signature set. Signatures of like plant types were aggregated into a single signature.

Producer's Accuracy (Errors of Omission)

Classification / *Reference Map*

	Erar	Ponu	Elma	Jubu	Psbr	Lisc	Plac
Erar	**126455**	1062	5574	0	9955	96	40
Ponu	5709	**487**	3389	0	73	674	514
Elma	13202	383	**28465**	0	214	10	96
Jubu	0	0	0	**0**	0	0	0
Psbr	34835	636	861	0	**6919**	231	61
Lisc	0	0	0	0	0	**0**	0
Plac	13985	187	10215	0	225	209	**1084**

Classification / *Reference Map*

	Erar	Ponu	Elma	Jubu	Psbr	Lisc	Plac
Erar	**65.12%**	38.55%	11.49%	0.00%	57.26%	7.87%	2.23%
Ponu	2.94%	**17.68%**	6.99%	0.00%	0.42%	55.25%	28.64%
Elma	6.80%	13.90%	**58.69%**	0.00%	1.23%	0.82%	5.35%
Jubu	0.00%	0.00%	0.00%	**0.00%**	0.00%	0.00%	0.00%
Psbr	17.94%	23.09%	1.78%	0.00%	**39.80%**	18.93%	3.40%
Lisc	0.00%	0.00%	0.00%	0.00%	0.00%	**0.00%**	0.00%
Plac	7.20%	6.79%	21.06%	0.00%	1.29%	17.13%	**60.39%**

User's Accuracy (Errors of Commission)

Reference Map / *Classification*

	Erar	Ponu	Elma	Jubu	Psbr	Lisc	Plac
Erar	**126455**	5709	13202	0	34835	0	13985
Ponu	1062	**487**	383	0	636	0	187
Elma	5574	3389	**28465**	0	861	0	10215
Jubu	0	0	0	**0**	0	0	0
Psbr	9955	73	214	0	**6919**	0	225
Lisc	96	674	10	0	231	**0**	209
Plac	40	514	96	0	61	0	**1084**

Reference Map / *Classification*

	Erar	Ponu	Elma	Jubu	Psbr	Lisc	Plac
Erar	**88.32%**	52.64%	31.16%	0.00%	80.00%	0.00%	53.99%
Ponu	0.74%	**4.49%**	0.90%	0.00%	1.46%	0.00%	0.72%
Elma	3.89%	31.25%	**67.18%**	0.00%	1.98%	0.00%	39.43%
Jubu	0.00%	0.00%	0.00%	**0.00%**	0.00%	0.00%	0.00%
Psbr	6.95%	0.67%	0.51%	0.00%	**15.89%**	0.00%	0.87%
Lisc	0.07%	6.21%	0.02%	0.00%	0.53%	**0.00%**	0.81%
Plac	0.03%	4.74%	0.23%	0.00%	0.14%	0.00%	**4.18%**

Overall Accuracy: 61.47%

5.2.5 Signature Evaluation with Vila, Aster, and Hefa

In addition to the spectral signatures generated for the supervised classifications, signatures were collected from Vila, aster, and Hefa plant types which were outside of the vernal pool basins. Signatures for these plants are given in Figure 19 with the signatures from the second supervised classification.

Transformed divergence (TD) measures provide an indication of the separability of spectral signatures. Values of 2000 indicate excellent between-class separation, values above 1900 indicate good separation, and values below 1700 indicate poor separation (Jensen, 1996). Transformed divergence measures were derived using the signatures in Figure 19. Most between-class separation values of TD were above 1900. However, the TD between Ponu and Plac was 912, between Erar and Aster was 1201, and between Psbr and Hefa was 1784. This indicates that that these classes are likely to have the greatest spectral confusion using semi-automated image classification.

5.3 Pool Water Depth

The red/blue spectral index demonstrated a potential, yet weak positive relationship with basin water depth, while the blue/NIR index and the NDVI had no relationship with water depth within the vernal pool basins. Scatterplots illustrating the spectral indices plotted against pool depth are given in Figure 20 through Figure 22. The R^2 values between the spectral indices and water depth were not statistically significant at 0.2387, 0.0114, and 0.0622 for the red/blue, blue/NIR, and NDVI spectral indices, respectively. These poor results are largely attributable to the shallow nature of the vernal pools and to the range of water turbidity and coloration within the pools at the Otay Mesa site. These indices seem to be related more strongly with water turbidity than with depth. Further, the apparent positive relationship between the red/blue index and depth is likely due to increasing suspended sediments as pool depth increases. However, this study did not have sufficient ground data on water turbidity within the basins to validate these assertions.

5.4 Mapping Land Use and Land Cover Near Vernal Pools

High spatial resolution, multispectral imagery may be utilized for mapping many land use/land cover types at as high of categorical detail as Level III and Level IV of the USGS classification system (Anderson et al., 1976). In the context of characterizing land use and land cover adjacent to vernal pools, high spatial resolution ADAR 5500 imagery may be utilized to interpret and map urban land use such as single and multiple family residential, commercial, industrial, and agriculture. As demonstrated through a San Diego State University NASA Affiliated Research Center (ARC) project, this type of imagery may also be utilized to interpret and classify southern California vegetation community types such as coastal sage scrub, chaparral, grassland, and disturbed variations of these classes (Coulter et al., 2000). In addition, disturbance features such as off-road vehicle activity and fire which increase the soil exposure are evident in high

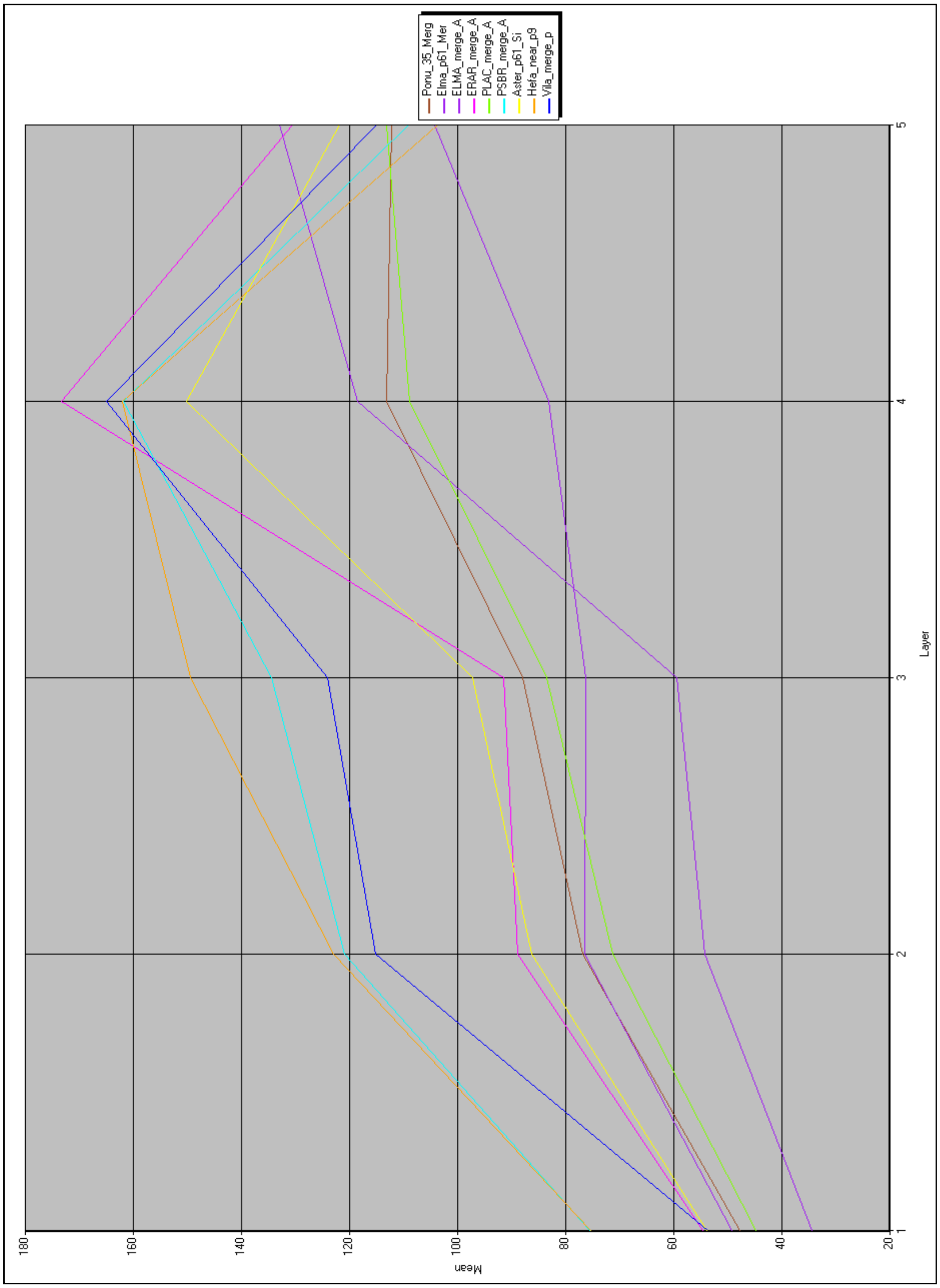

Figure 19. Spectral signatures from the second supervised classification signature set with Vila, aster, and Hefa. NDVI is represented as layer 5.

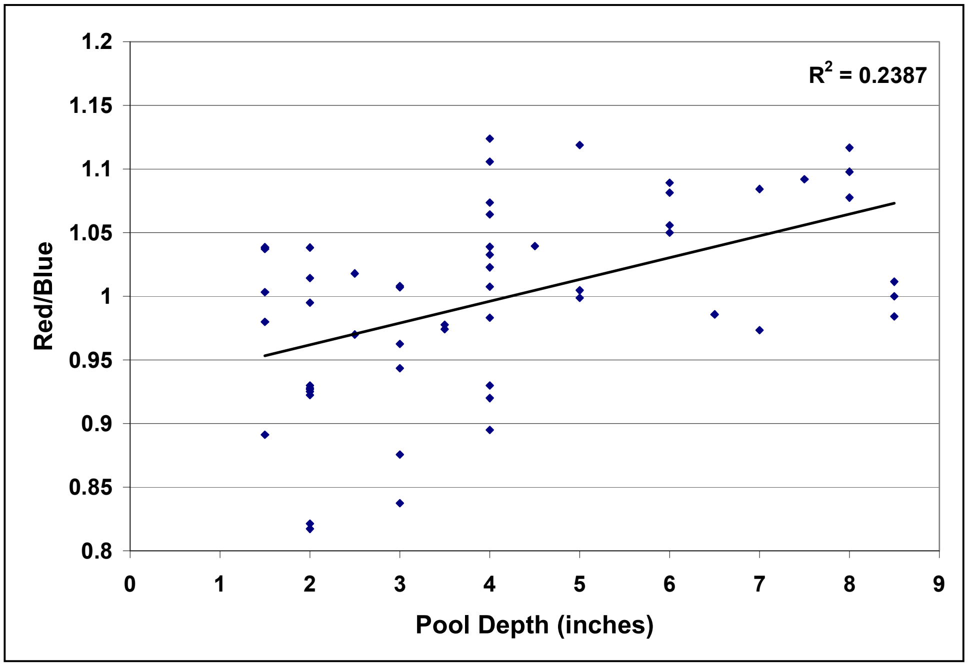

Figure 20. Scatterplot of red/blue index values plotted against pool depth.

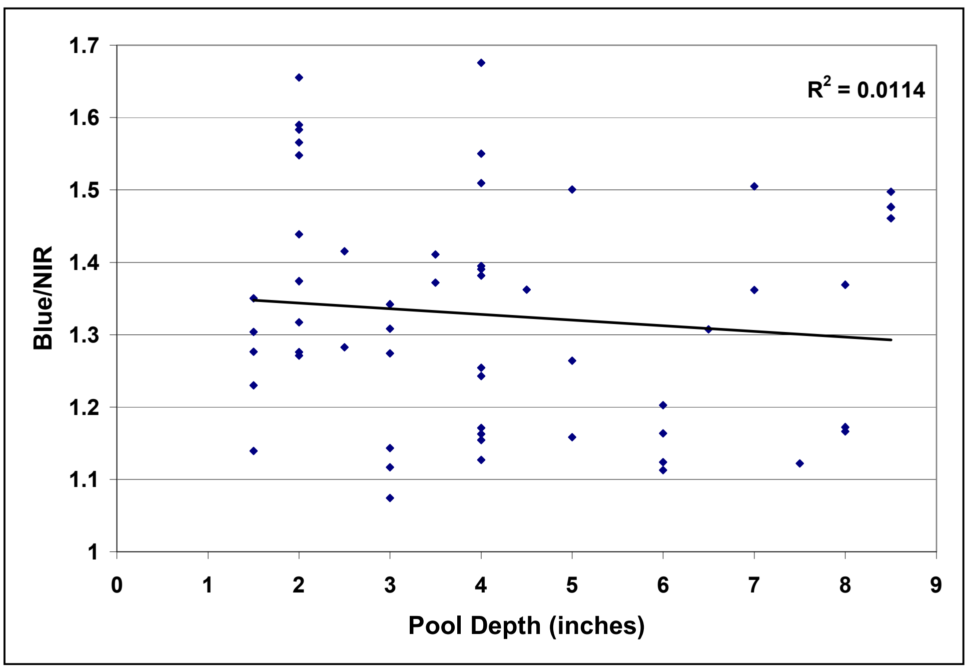

Figure 21. Scatterplot of blue/near-infrared index values plotted against pool depth.

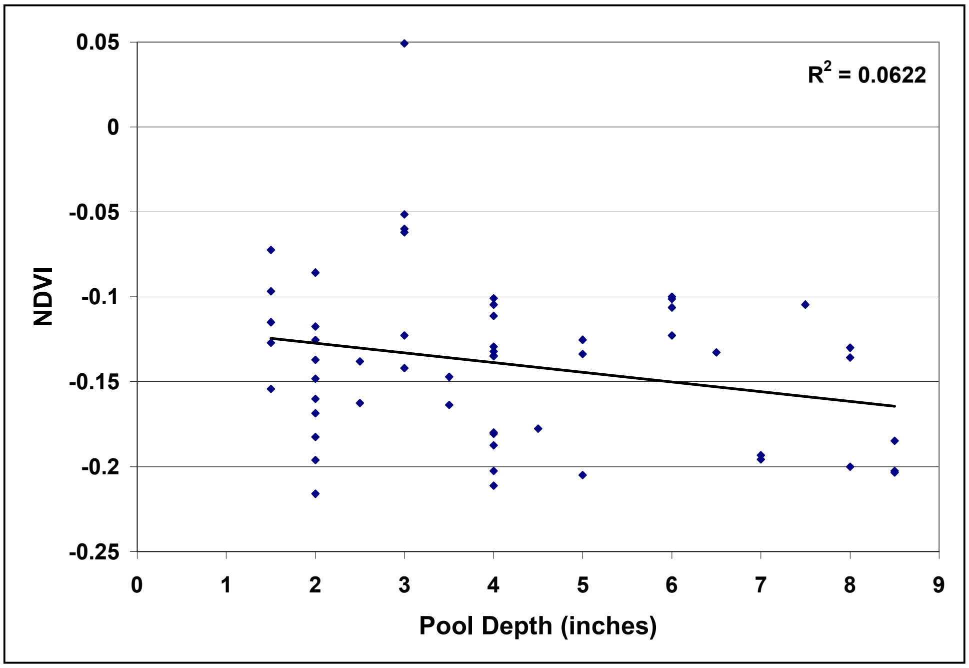

Figure 22. Scatterplot of NDVI index values plotted against pool depth.

resolution ADAR imagery. Classification of these land cover features is best performed through visual interpretation. However, semi-automated image classification may provide sufficiently accurate maps characterizing land use and land cover adjacent to vernal pools.

ADAR 5500 imagery utilized during this project was inspected for information content on watershed boundaries and mima mound locations adjacent to vernal pools. Some mima mounds were apparent in the 2 inch resolution imagery at Otay Mesa. This is largely due to the sparse vegetation cover atop the mima mounds at the restored Otay Mesa site. Interpretation of mima mounds is not likely to be successful in areas of mature and native vernal pools. Watershed boundaries were not apparent in the imagery and are not likely to be interpretable. It is possible that watershed boundaries may be derived through a photogrammetric process with stereo imagery. However, this process would greatly increase costs and the resulting accuracy in vernal pool landscapes with minimal relief is questionable.

6.0 Cost/Benefit Analysis

Results from this study suggest that the greatest utility of remote sensing for vernal pool assessment is locating and delineating unknown pools across large extents of the City of San Diego. However, the real utility of remote sensing for deriving the information of interest is also a function of cost savings associated with mapping, compared to more conventional field-based methods. If a remote sensing approach is to be implemented, it must be cost-effective relative to alternative methods of locating and delineating unknown vernal pools, such as field-based mapping.

A comparative analysis of image-based and field-based mapping was performed to assess the relative cost-effectiveness of the two approaches. Estimates of image-based mapping costs were generated by compiling pricing information for: ADAR 5500 aerial imagery at 2 ft and 4 ft resolution, Emerge aerial imagery at 2 ft and 4 ft resolution, Quickbird satellite imagery at 8 ft (2.4 m) resolution, and IKONOS satellite imagery at 13.12 ft (4 m) resolution. In addition to image acquisition and georeferencing costs, costs associated with locating and delineating vernal pools through image interpretation were estimated.

Estimates of image-based mapping costs were compared to ground-based mapping costs provided by the City of San Diego from two City projects. For the first, a consultant was paid \$2520 to delineate known vernal pool basin perimeters within a 0.02 hectare area using GPS. At this rate of \$1260 per hectare, it would cost \$126,000 to map 1 km^2 using this consultant. For the purpose of our analysis, we assumed that economies of scale would allow the consultant to map 1 km^2 at 80% of the per-unit area cost for the 0.02 hectare area, or for approximately \$100,000. For the second project, a \$257,276 grant was obtained by the City to cover costs associated with locating unknown vernal pool basins within a 70 km^2 area and delineating basin perimeters using GPS.

For the comparative analysis, image-based mapping costs were estimated for the 70 km^2 area and compared to those associated with the field-based mapping across the same extent. Image-based mapping costs were also computed on a per-square kilometer basis (by dividing the final cost estimate by 70) and compared to the ground-based cost of a consultant to map 1 km^2. Results from the analysis are given in Table 7. Accuracy measures listed in Table 7 for detecting and delineating pools are based upon the Otay Mesa results from the analysis of the optimum spatial resolution for pool detection.

ADAR product costs at 70 km^2 assume 30% sidelap and 30% endlap between frames and semi-automated georeferencing using DIME software produced by Positive Systems, Inc. of Whitefish, Montana. DIME users are charged a \$5.00 fee for every georeferenced ADAR 5500 image output from DIME. Therefore, these fees were included in the totals. Acquisition and georeferencing costs for the 2 ft resolution ADAR were calculated by assuming: four hours of flight time at \$2000 per hour (includes planning, flight prep, crew time, ADAR system costs, and post-processing); plus 0.25 hours per frame to georeference, times 4 frames/km^2, times 70 km^2 area, times \$75 per hour for consultant fees; plus \$5 per frame DIME charge, times 4

Table 7. Image-based and ground-based pool identification and delineation costs.

Spatial Resolution	Sensor	Pool Identification/ Locating Accuracy	Image Acquisition and Georeferencing Cost for 70 km^2	Image Acquisition, Georeferencing, and Pool Delineation Cost for 70 km^2	Image Acquisition, Georeferencing, and Pool Delineation Cost per 1 km^2
2 ft	ADAR	80%	$14,650.00	$19,900.00	$284.29
4 ft	ADAR	70%	$5662.50	$10,912.00	$155.89
2 ft	Emerge	NT	$8000.00	$13,250.00	$189.29
4 ft	Emerge	NT	$8000.00	$13,250.00	$189.29
8 ft (2.4 m)	Quickbird XS	60%	$2730.00	$7,980.00	$114.00
13.12 ft (4 m)	IKONOS XS	20%	$2030.00	$7,280.00	$104.00
Ground-Based		??		$257,276.00	$100,000.00

NT: Indicates that comparable imagery was not tested.

frames/km^2, times 70 km^2 area. Calculation of 2 ft ADAR acquisition and georeferencing costs is summarized in Equation 2.

$$(4 \text{ hrs} * \$2000/\text{hr}) + (0.25 \text{ hrs} * 4 \text{ frames/km}^2 * 70 \text{ km}^2 * \$75/\text{hr}) + (\$5 * 4 \text{ frames/km}^2 * 70 \text{ km}^2) = \$14,650.00 \quad \text{(Equation 2)}$$

Acquisition and georeferencing costs for the 4 ft resolution ADAR were based upon: two hours of flight time at $2000.00 per hour; plus 0.25 hours per frame to georeference, times 1_frame/km^2, times 70 km^2 area, times $75 per hour; plus $5 per frame DIME charge, times 1_frames/km^2, times 70 km^2 area. Calculation of 4 ft ADAR acquisition and georeferencing costs is summarized in Equation 3.

$$(2 \text{ hrs} * \$2000/\text{hr}) + (0.25 \text{ hrs} * 1 \text{ frame/km}^2 * 70 \text{ km}^2 * \$75/\text{hr}) + (\$5 * 1 \text{ frame/km}^2 * 70 \text{ km}^2) = \$5662.50 \quad \text{(Equation 3)}$$

It was estimated that detecting and delineating pools would require approximately one hour of image interpretation per square kilometer and that a consultant would charge $75 per hour for this service. Therefore, a total of $5250 was added to the image acquisition and georeferencing costs to account for pool locating and delineation across the 70 km^2 area. This same cost for detecting and delineating vernal pools was assumed for each of the imagery types.

Image acquisition and georeferencing costs for Emerge were based upon a single day of acquisition. Emerge quoted a range of $8000.00 to $10,000 per day for any project. As 70 km^2 is a relatively small area to cover in a single day, $8,000 was maintained as the total cost for acquisition and georeferencing. Emerge also indicated that imagery at 2 ft resolution would cost the same as imagery at a lower spatial resolution. Therefore, acquisition and georeferencing costs for the Emerge imagery are the same at 2 ft and 4 ft spatial resolution. Emerge is able to offer a range of spatial resolutions at the same cost due to the larger image array relative to the ADAR 5500 system. The Emerge camera array is 2000 x 3000 pixels, while the ADAR 5500 array is 1000 x 1500 pixels. However, the Emerge camera sub-samples three wavebands of data onto a single chip and cannot offer true multispectral data, as no two wavebands are directly sampled for any pixel. For this reason, pool identification/locating accuracy is not reported in Table 7 for Emerge imagery, as it is uncertain that identification accuracy with 2 and 4 ft resolution sub-sampled imagery will be comparable to accuracy obtained with the ADAR 5500.

Quickbird and IKONOS costs are based upon imagery with positional accuracy suitable for mapping at 1:50,000 scale (comparable to the ADAR and Emerge products). For 1:50,000 scale positional accuracy, Quickbird imagery is \$39/km^2 while IKONOS imagery is \$29/km^2.

Results from the analysis of image and ground-based costs indicate that locating and delineating vernal pools through remote sensing could be significantly more cost-effective than ground-based mapping. Mapping vernal pools across a 70 km^2 area is estimated to be less than one-tenth of the cost of ground-based mapping. While extrapolation of ground-based mapping costs from a 0.02 km^2 area to a 1 km^2 area may not be entirely realistic, it seems clear that mapping vernal pools at the scale of kilometers will be most cost-effective through remote sensing.

7.0 Conclusions

The utility of high spatial resolution, multispectral imagery was evaluated for multiple tasks associated with vernal pool mapping and characterization, including: 1) locating unknown pools and delineating pool basin extents; 2) mapping vernal pool plants; 3) estimating pool depth; and 4) characterizing land use and land cover adjacent to sensitive vernal pool habitats. Acquisition of remotely sensed imagery enables synoptic and large area coverage of land cover conditions from a birds-eye view. Further, remotely sensed imagery provides a record of land cover distribution and patterns at the time of acquisition. The greatest utility of remote sensing for vernal pool management is likely to be in locating and mapping vernal pools and in documenting and characterizing land cover conditions within and adjacent to the pools. These conditions include: general vegetation type; disturbances such as off-road vehicle activity, and urban land use.

Results from the analysis of the optimum spatial resolution for detecting and delineating pools indicate that imagery on the order of 2 ft spatial resolution has the highest accuracy for identifying vernal pools and delineating basin extents. Pool detection accuracy was 80% at the Otay Mesa site. However, this accuracy is expected to improve with greater familiarity and experience in interpreting vernal pools. In addition, viewing of additional image products such as the blue/NIR ratio and the NDVI will likely improve interpretation accuracy. During the course of the project, one previously unknown vernal pool at Marron Valley was identified and field validated.

Within 2 ft resolution imagery, the perimeter of vernal pool basins with ponded water is generally apparent and likely to be mapped with 2 ft to 4 ft precision. Dry pool basins are likely to be delineated with lower precision. In all cases, pool detection and delineation is influenced by pool size, color, contrast to background, and vegetation within and surrounding the pools.

Semi-automated image classification yielded species maps with 60-75% accuracy for Erar and Elma. Classification accuracy was generally low for Ponu, Psbr, Lisc, and Plac classes. Ponu and Plac were found to have very similar spectral responses. Ponu also demonstrated some spectral overlap with Elma and Erar. In addition, Erar generally demonstrated some degree of spectral overlap with all plant types mapped.

Image classification results suggest that image-based mapping of most vernal pool plants may not be sufficiently accurate and reliable for operational inventorying of vernal pool flora. However, image classification results for the Ponu, Lisc, and Plac classes were significantly influenced by the small extent mapped as reference and the few samples from which spectral signatures could be extracted. In addition, reference polygons were coarsely delineated at the few locations of Ponu and Lisc and classification accuracy would likely be improved given more precise delineation of homogenous plant cover within reference polygons for these classes. Therefore, the classification accuracy results for these classes should not be viewed as definitive. Future research in this area should include more complete and representative ground sampling of plants for validation of image classifications.

Relationships between water depth and the spectral index products evaluated were weak or non-existent. Therefore, estimates of pool depth are not likely to be derived from high spatial resolution, multispectral imagery. However, differences in pool depth over time may be indicated by expansion or contraction of pool basin perimeters.

The comparative analysis of image-based and field-based mapping costs indicate that projects at or above spatial extents of a few kilometers are likely to be most cost-effective through remote sensing. For a 70 km^2 project, image-based mapping costs were estimated to be less than one-tenth of ground-based pool locating and mapping costs. At the scale of a single square kilometer, image-based mapping estimates were less than those extrapolated from a ground-based survey over a 0.02 km^2 area. However, direct extrapolation of the field-based costs from the 0.02 km^2 project to a 1 km^2 project may over-estimate costs.

8.0 References

Anderson, J. R., E. E. Hardy, J. T. Roach, and R. E. Witmer. 1976. A land use and land cover classification system for use with remote sensor data. *Geological Survey Professional Paper 964*, U.S. Government Printing Office, Washington, D.C., 28 p.

Bauder, E. T. 1986. San Diego vernal pools: Recent and projected losses; their condition; and threats to their existence, 1979-1990. Report prepared for Endangered Plant Project, California Department of Fish and Game, Sacramento, CA.

Bauder, E. T. 1987. Threats to San Diego vernal pools and a case study in altered pool hydrology. In T. S. Elias, ed., Conservation and management of rare and endangered plants, California Native Plant Society, Sacramento, CA., pp 209-213.

Bauder, E. T. and S. McMillan. 1998. Current distribution and historical extent of vernal pools in Southern California and Baja California, Mexico. In C. W. Witham, E. T. Bauder, D. Belk, W. R. Ferren Jr., and R. Ornduff, eds. Ecology, Conservation, and Management of Vernal Pool Ecosystems - Proceedings from a 1996 Conference, California Native Plant Society, Sacramento, CA., pp 56-70.

Beauchamp, M. 1979. Survey of vernal pools of Kearny Mesa, San Diego County, Spring 1979. Principal investigators: P. H. Zedler, T. A. Ebert; research associate, M. Lee Balko ; consultant, R. Mitchel. Beauchamp Publisher.

Coulter, L, D. Stow, A. Hope, J. O'Leary, D. Turner, P. Longmire, S. Peterson, and J. Kaiser. 2000. Comparison of high spatial resolution imagery for efficient generation of GIS vegetation layers. *Photogrammetric Engineering and Remote Sensing*, 66 (11), pp 1329-1335.

Jenson, J. R. 1996. Introductory Digital Image Processing, a remote sensing perspective, second edition. Prentice Hall, Upper Saddle River, NJ.

Lathrop, R. G., T. M. Lillesand, and B. S. Yandell. 1991. Testing the utility of simple mult-date Thematic Mapper calibration algorithms for monitoring turbid inland waters. *International Journal of Remote Sensing*, 12(10), pp 2045-203.

City of San Diego, California and U. S. Fish and Wildlife Service. 1997. Final EIR/EIS, issuance of take authorizations for threatened and endangered species due to urban growth within the Multiple Species Conservation Program (MSCP) planning area, San Diego, CA.

U. S. Fish and Wildlife Service. 1997. Environmental assessment and land protection plan: Vernal pools stewardship project, San Diego National Wildlife Refuge, San Diego, CA., Portland, OR.